

PARABOLIC REPRESENTATIONS AND GENERALIZED RILEY POLYNOMIALS

YUNHI CHO, HYUK KIM, SEONHWA KIM, AND SEOKBEOM YOON

ABSTRACT. We generalize R. Riley’s study about parabolic representations of two bridge knot groups to the general knots in S^3 . We utilize the parabolic quandle method for general knot diagrams and adopt symplectic quandle for better investigation. For any knot diagram with a specified crossing c , we define a generalized Riley polynomial $R_c(y) \in \mathbb{Q}[y]$ whose roots correspond to the conjugacy classes of parabolic representations of the knot group. The *sign-type* of parabolic quandle is newly introduced and we obtain a formula for the obstruction class to lift a boundary unipotent $SL_2\mathbb{C}$ -representation. Moreover, we define another polynomial $g_c(u) \in \mathbb{Q}[u]$, called u -polynomial, and prove that $R_c(u^2) = \pm g_c(u)g_c(-u)$. Based on this result, we introduce *Riley field* and *u-field* which are closely related to the invariant trace field. Finally, we present thorough computations of parabolic representations by our method for the examples of knots, 4_1 , 7_4 , 8_{18} , 9_{29} , and the link 5_1^2 , along with the complex volume and cusp shape for each representation.

CONTENTS

1. Introduction	2
1.1. Backgrounds about parabolic representations	2
1.2. Parabolic quandles and Riley polynomials	3
1.3. Sign-types and obstruction classes	4
1.4. u -polynomials and their properties	4
1.5. Riley field, u -field, and trace field	5
1.6. Homomorphisms between knot groups	5
1.7. Computations	5
1.8. 8_{18} knot	6
1.9. Final remark	6
Acknowledgments	7
2. Preliminaries	7

(Y.Cho) DEPARTMENT OF MATHEMATICS, UNIVERSITY OF SEOUL, SEOUL, 02504, KOREA (KOREA INSTITUTE FOR ADVANCE STUDY, SEOUL, 02455, KOREA)

(H.Kim) DEPARTMENT OF MATHEMATICAL SCIENCES, SEOUL NATIONAL UNIVERSITY, SEOUL, 08826, KOREA

(S.Kim) DEPARTMENT OF MATHEMATICS, NATURAL SCIENCE RESEARCH INSTITUTE, UNIVERSITY OF SEOUL, 02504, SEOUL, KOREA

(S.Yoon) DEPARTAMENT DE MATEMÀTIQUES, UNIVERSITAT AUTÒNOMA DE BARCELONA, 08193 CERDANYOLA DEL VALLÈS, SPAIN

E-mail addresses: (Y.Cho) yhcho@uos.ac.kr, (H.Kim) hyukkim@snu.ac.kr, (S.Kim) seonhwa17kim@gmail.com, (S.Yoon) sbyoon15@gmail.com.

Date: April 4, 2022.

2.1. Parabolic representation	7
2.2. Character variety	8
2.3. Parabolic quandle	10
2.4. Symplectic quandle	12
2.5. Riley polynomial	13
3. Parabolic quandle with sign-type	14
3.1. Sign-types	14
3.2. Total-sign	15
3.3. Obstruction classes	16
3.4. Parabolic representations	17
3.5. Normalization	19
4. Riley polynomial and u -polynomial	19
4.1. Generalized Riley polynomial	19
4.2. y -value and u -value	21
4.3. u -polynomials	22
4.4. u -polynomial and sign-types	23
5. Trace field	25
5.1. Invariant trace fields	25
5.2. Riley field, u -field, and trace field	26
6. Homomorphisms between knot groups	28
7. Computations	29
7.1. 4_1 knot	30
7.2. 7_4 knot	32
7.3. 9_{29} knot	35
7.4. Computations for links: 5_1^2 Whitehead link	39
8. Computation of $X_{par}(8_{18})$ and diagrammatic Symmetry	42
8.1. Computation	42
8.2. $X_{par}(8_{18})$ and complex volume	46
References	49

1. INTRODUCTION

1.1. Backgrounds about parabolic representations. Parabolic representations of two bridge links were intensively studied by R. Riley in the '70s [Ril72, Ril75] and his far-reaching computations produced lots of discrete faithful representations of the knot groups, which contributed to the earlier development of 3-dimensional geometry and topology by W. Thurston [Thu77, Ril13]. A *parabolic representation* of a knot group is an $SL_2\mathbb{C}$ or $PSL_2\mathbb{C}$ representation which sends a meridian to a parabolic element. The parabolicity condition is algebraically the same as the completeness condition of Thurston gluing equations for a complete (pseudo-) hyperbolic structure.

One advantage of boundary-parabolic representations is that complex volume is well-defined [Neu04, Zic09]. The Chern-Simons invariant for any $SL_2\mathbb{C}$ -representation has a subtle ambiguity to be defined and requires additional data about a logarithmic branch in the boundary [Mar12] although the hyperbolic volume is defined regardless of the boundary condition [Fra04].

Parabolic representations naturally produce elements in the extended Bloch group coming from the image of the fundamental class of knot exterior, and hence the volumes of parabolic representations would be related to Neumann's conjecture [Neu11]. Arithmetic invariants like the invariant trace field and quaternion algebras [MR03] can be also defined for any parabolic representation just as for the holonomy of a complete hyperbolic manifold of finite volume. These arithmetic invariants have been well-studied for the past several decades, in particular, with the aid of computer software like SnapPy. Our work is an extension of these previous studies of the holonomy representation to general parabolic representations and provides a diagrammatic framework that allows us various examinations and computations directly related to a knot diagram.

On the other hand, parabolic representations naturally appear in the study of the volume conjecture [MY18]. An optimistic limit of a colored Jones polynomial (resp. Kashaev invariant) is a critical value of a potential function $W(w_1, \dots, w_{N+2})$ (resp. $V(z_1, \dots, z_{2N})$) made up of dilogarithm function Li_2 , where w_i (resp. z_i) $\in \mathbb{C} \setminus \{0\}$ and N is the number of crossings in the diagram. Here, parabolic representations are given as the critical points of $W(w)$ (resp. $V(z)$) since they are solutions to Thurston gluing equation of the corresponding ideal triangulation called *octahedral decomposition*. A remarkable point is that the diagrammatic formulas for the explicit computation of parabolic representations as well as their hyperbolic invariants can be derived in this setting. For example, in [CM13, CKK14, KKY18], complex volume, cusp shape, and Wirtinger presentation matrices are obtained in terms of z - or w -variables suggesting the direct connection to quantum invariants. Cho and Murakami [CM13, Cho16a, Cho18] express these w -variables or z -variables by using parabolic quandle for vector coloring introduced by A. Inoue and Y. Kabaya [IK13]. Moreover, Ptolemy coordinates [Zic09] of octahedral decomposition for parabolic representations can also be described by these z - or w -variables [KKY19]. One of the themes in this paper is to study further from these previous works for parabolic representation and their invariants by considering parabolic quandle (see Section 2.3 for the definition) generalizing Riley's works on 2-bridge links to arbitrary links.

1.2. Parabolic quandles and Riley polynomials. The system of parabolic quandle equations in [IK13, JK20] is essentially equivalent to that of the Wirtinger relation, but is simpler and has a different flavor. It may be more tractable and interesting as we can reduce it to a symplectic quandle. From this consideration, Jo and Kim have employed such an idea for the case of two bridge links [JK20, JK22]. They not only reproduce Riley's results but also find some new algebraic properties of the Riley polynomial. In particular, in [JK20, Theorem 5.1] they showed that the Riley polynomial admits a *square-splitting* property, that is, $R(u^2) = \pm g(u)g(-u)$ for some $g \in \mathbb{Z}[u]$. One of the motivations of this paper is to answer the question of whether the square-splitting property holds for general knots not just restricted to two-bridge knots.

To do this, we first introduce a generalization of Riley polynomial to non-two-bridge cases. We observe that the roots of Riley polynomial $R(y)$ are nothing but a trace of $\rho(m_1 m_2)$ where ρ is a parabolic representation and m_1 and m_2 are the two meridians at the top-most(or

bottom-most) crossing in Conway normal form. Riley proved that $R(y)$ has distinct roots and hence there is a natural bijection between the set of roots of $R(y)$ and conjugacy classes of parabolic representations.

A two bridge diagram (of Conway form) has a kind of canonical choice of crossing i.e., the bottom-most or the top-most crossing. However, there is no canonical choice of a crossing in general link diagram and hence we just consider a knot diagram D_c with a specified *base crossing* c . Then we define *generalized Riley polynomial* $R_c(y)$ for D_c to be a polynomial whose roots are the trace of $\rho(m_i m_j)$ where m_i and m_j are two arcs at the based crossing c .

By a simple calculation (see Lemma 4.6), we can observe that each root of $R_c(y)$ is the square of the determinant of two parabolic quandle coloring vectors at the crossing c . It naturally follows that $R_c(u^2)$ can be written in the form of $g_c(u)g_c(-u)$. Thus, the natural question arises whether $R_c(u^2)$ splits in $\mathbb{Q}[u]$. It turns out that $g(u)$ has rational coefficients only for knots and we can check this does not hold for link examples (see Section 7.4).

1.3. Sign-types and obstruction classes. To clarify when $g_c(u)$ has rational coefficients, we study a more precise relation between the system of parabolic quandle equations and parabolic representations. The natural correspondence between parabolic quandles and Wirtinger generators has a certain sign-ambiguity, but we can obtain an unambiguous solution to the quandle equation by introducing a *sign-type* as follows.

Let the sign of each coloring vector be fixed. Then we define a *sign-type* ϵ of the parabolic quandle that is a sign-assignment at each crossing, i.e.,

$$\epsilon : \{ \text{crossings in } D \} \longrightarrow \{\pm 1\},$$

which is the sign of the quandle equation at each crossing in Definition 3.1. Then, we obtain that the product of $\epsilon(i)$ over all crossings doesn't depend on the choice of the sign-type (Proposition 3.5). It would be natural to ask what the unchanged value is. We prove that it coincides with *obstruction class* $\varepsilon(\rho)$ of the associated representation ρ in Theorem 3.8 as follows,

$$\varepsilon(\rho) = \prod_{c \in \text{crossings}} \epsilon(c) = \text{the eigen value of a longitude.}$$

In other words, it determines whether ρ (or a lifting of $\text{PSL}_2\mathbb{C}$ -representation ρ) is a boundary-unipotent $\text{SL}_2\mathbb{C}$ -representation or not.

Remark that 9_{29} admits a parabolic representation of positive obstruction. See the computation in Section 7.3. As looking at the datasets of [GKR⁺] and [CK], we can observe that almost all parabolic representations have negative obstruction. It turned out that the geometric representation must have negative obstruction [Cal06].

1.4. u -polynomials and their properties. Furthermore, if we fix any sign-type ϵ for a knot diagram then we have an exact bijection between the conjugacy classes of parabolic representations and the solution of parabolic quandle equation with the obstruction ε . Based on this setting, we can prove that $g_c(u)$ has \mathbb{Q} -coefficients by elementary Galois theory and we call $g_c(u)$ *u -polynomial*. As an immediate corollary, we prove the square-splitting property of generalized Riley polynomial, i.e. $R_c(u^2) = \pm g_c(u)g_c(-u)$ with $g(u) \in \mathbb{Q}[u]$.

We remark the u -polynomial has more information than Riley polynomial when the generalized Riley polynomial is reducible. Let us suppose $R(y) = R_1(y)R_2(y)$, then we have the corresponding $g(u) = g_1(u)g_2(u)$ with $R_i(u^2) = \pm g_i(u)g_i(-u)$ for $i = 1, 2$. But the choice of individual $g_i(u)$ or $\pm g_i(-u)$ for each i cannot be chosen arbitrarily since all factors of $g_i(u)$ are affected simultaneously as we change the sign-type. Hence we have a subtle “sign-coupling” phenomenon interrelating irreducible factors of $g(u)$. At the moment the meaning of this coupling is not clear but this is quite remarkable since the interrelation between all irreducible components of a character variety is rare, while many known properties about a character variety are essentially related to a single irreducible component. It would be interesting if the sign-coupling phenomenon can be revealed in a further study. Remark that another example interrelating all irreducible components of character variety is the vanishing property of adjoint Reidemeister torsion. See [GKY19],[TY21].

1.5. Riley field, u -field, and trace field. Instead of choosing a base crossing c , a Riley polynomial $R_{ij}(y)$ (resp. u -polynomial $g_{ij}(u)$) can be naturally considered for a pair of arcs a_i and a_j as well. Similarly, each root of $R_{ij}(y)$ (resp. $g_{ij}(u)$) corresponds to a parabolic representation ρ and hence we define *Riley field* (resp. *u -field*) of ρ as the number field $\mathbb{Q}(\{y_{ij}\})$ (resp. $\mathbb{Q}(\{u_{ij}\})$) generated by the corresponding y_{ij} 's (resp. u_{ij} 's) over all pairs of arcs.

At first glance, the Riley field seems to be a more natural object than the u -field since the generators are the traces of all words of length two. An obvious fact is that $\mathbb{Q}(\{y_{ij}\})$ is a subfield of $\mathbb{Q}(\text{tr } \rho)$, but it seems to be difficult to see whether it is a knot invariant or how it is related to the trace field $\mathbb{Q}(\text{tr } \rho)$. However, in contrast to the Riley field, it can be naturally proved that $\mathbb{Q}(\{u_{ij}\})$ is a knot invariant and $\mathbb{Q}(\{u_{ij}\}) \supset \mathbb{Q}(\text{tr } \rho)$ (see Theorem 5.2 and Theorem 5.3.). Therefore, the u -field seems to be a better object to study than the Riley field.

Based on a lot of computer experiments, we conjecture that the u -field is always the same as the Riley field (see Conjecture 2 and Conjecture 3). If the conjecture is true, then the Riley fields, u -field, and the trace field, all three are identical and in particular, the trace field is generated by only the words of length two, which is a special property of parabolic representation of a knot group. It could be quite surprising because the trace relation usually requires the word of length three.

1.6. Homomorphisms between knot groups. An interesting application is that Riley polynomial gives a necessary condition to admit a homomorphism $\phi : \pi_1 K \rightarrow \pi_1 K'$ such that $\phi(\alpha_c) = \alpha_{c'}$ for a crossing loop α_c of K and $\alpha_{c'}$ of K' . If there is such a homomorphism then each irreducible factor of $R'_c(y)$ should divide $R_c(y)$. In particular, $R_{c'}(y) \mid R_c(y)$ if ϕ is an epimorphism and $R_{c'}(y) = R_c(y)$ if ϕ is an automorphism. This result may help study epimorphism or automorphism between knot groups, in particular, for meridian preserving cases.

1.7. Computations. We give several expository computations as examples by using parabolic quandle for the cases of 4_1 , 7_4 , 8_{18} , 9_{29} , and 5_1^2 (Whitehead link). We provide a detailed

procedure to obtain a complete list of parabolic representations and compute their obstruction classes, Riley polynomials, and u -polynomials. The complex volumes and cusp shapes are also computed numerically by a new diagrammatic method developed recently, which is inspired by the volume conjecture ([CKK14], [Cho16b], [KKY18], [KKY19]). All these computations are cross-checked by SnapPy [CDGW] and CURVE project [GKR⁺] data.

Remark that Chern-Simons invariants in the CURVE project are only computed modulo $\frac{\pi^2}{6}$ but our computation is modulo π^2 as the Chern-Simons invariant is originally defined by modulo π^2 . Moreover, we stress that the list of parabolic representations by our method is complete, i.e. there is no missing irreducible representation. For example, we found that 9_{29} knot has a representation of positive obstruction which is missing in the CURVE project.

The 7_4 is the first example which has two irreducible components of X_{par} , *the character variety of parabolic representations*, and moreover, we give an example of a generalized Riley polynomial whose constant term is not ± 1 . The 9_{29} is known as the first example having a non-integral trace [RR21]. Note that non-integral Riley polynomial for this example also provides a non-integral trace.

Remark that, in the case of 4_1 , 7_4 , and 5_1^2 , we can compute X_{par} essentially by hands without the aid of a computer since it uses only long-division of polynomials of small degree. But the other examples require the aid of an elimination algorithm like Gröbner basis to solve the system.

The computation method works for link cases as well. But the square-splitting property doesn't hold for link cases and we can see this for the case of Whitehead link 5_1^2 . We point out several differences for link cases with the 5_1^2 example in Section 7.4.

1.8. 8_{18} knot. In the case of 8_{18} , the structure of X_{par} is fairly complicated and the whole set of the parabolic representations is not known yet so far. Although the CURVE project [GKR⁺] provides a list of parabolic representations of 8_{18} , it contains only 20 representations. By our method, we assert that *there are exactly 26 parabolic representations up to conjugation*. Furthermore, we verify that the Riley polynomials at each crossing respect the rich symmetry of the 8_{18} diagram by the necessary condition of Riley polynomials in Theorem 6.4 to admit a knot group automorphism. Using these together, we obtain that 8_{18} has essentially different 12 parabolic representations and they are completely classified by the complex volumes. See Theorem 8.3.

1.9. Final remark. We would like to highlight that the parabolic quandle system in this paper provides a very efficient system of equations to obtain all parabolic representations. For example, if one tries to solve the system of equation directly from the Wirtinger relation of 8_{18} , it would be quite difficult even with the help of a computer. Note that Thurston gluing equation used by SnapPEA is much more efficient to solve by computer but it never guarantees that all parabolic representations are obtained. The parabolic quandle method in this paper, however, can compute the complete list of parabolic representations for 8_{18} easily by a low-performance laptop. In a subsequent paper, we will provide a complete list of parabolic representations for the whole Rolfsen knot table and beyond. The ongoing computational data can be accessed in [CK]

Moreover, the parabolic quandle method studied in this paper is not only effective but also conceptually interesting, as can be seen in the advent of sign-type or u -field. Moreover, these approaches using quandle vector can be generalized to non-parabolic representations and still produce an effective system to solve and it helps to understand the whole representation variety, character variety, and A -polynomial. We will see these studies in the forthcoming papers.

Finally, we ask a basic and fundamental question on the existence of parabolic representations of knot group. For irreducible $SU(2)$ -representations (and hence irreducible $SL_2\mathbb{C}$ -representations as well), its existence for any nontrivial knot is known due to Kronheimer and Mrowka [KM04]. On the other hand, the existence of (non-abelian) parabolic representation seems not to be discussed yet in the literature despite its fundamental importance. We formulate the following conjecture in a little stronger statement.

Conjecture 1. A knot K is nontrivial if and only if $X_{par}(K)$ is nonempty. Furthermore it has a zero-dimensional component.

This question looks quite plausible and is true for all the known computations.

ACKNOWLEDGMENTS

The authors express their gratitude to Professor Dong-il Lee at Seoul Women's University for consulting about Groebner basis technique, Dr. Dong Uk Lee for the valuable comments about algebraic and arithmetic geometry, and Phillip Choi for computer calculation support. The work of YC was supported by the 2021 sabbatical year research grant of the University of Seoul. The work of HK and SK was supported by the National Research Foundation of Korea (NRF) grant funded by the Korean government (MSIT) respectively (NRF-2018R1A2B6005691) and (No. 2019R1C1C1003383).

2. PRELIMINARIES

Let us review some basic definitions and facts to set the notation and terminology in this paper. We will follow common usage in most textbooks if the precise definition is not given here.

Let K be an oriented knot in S^3 . A *knot group* $\pi_1 K$ is the fundamental group $\pi_1(S^3 \setminus K)$ of the knot complement $S^3 \setminus K$. Sometimes we deal with links in S^3 , but we always consider only knots unless specified. Let D be an oriented knot diagram of K with N crossings. Let $c_1 \dots c_N$ denote the crossings in D and a_1, \dots, a_N denote the arcs, where an *arc* (i.e., *over-arc*) is a connected curve of D between two under-passing crossings, that is through only over-passing crossings.

2.1. Parabolic representation. *Wirtinger presentation* of $\pi_1 K$ is a well-known diagrammatic group presentation for a given D defined as

$$\pi_1 K = \langle m_1, \dots, m_N \mid r_1, \dots, r_N \rangle,$$

where the generators m_i are meridian loops corresponding to each arc a_i , and the relators r_n corresponding to each crossing c_n are given as in Figure 1 as usual.

$$\begin{array}{ccc}
& \xrightarrow{\quad m_i \quad} & a_i, \\
\begin{array}{c} \diagup \quad \diagdown \\ c_n \quad a_j \\ \diagdown \quad \diagup \\ a_i \quad a_k \end{array} & : r_n = m_j^{-1} m_k^{-1} m_i m_k, & \begin{array}{c} \diagup \quad \diagdown \\ a_i \quad c_n \quad a_k \\ \diagdown \quad \diagup \\ a_j \end{array} : r_n = m_j^{-1} m_k m_i m_k^{-1}
\end{array}$$

FIGURE 1. Wirtinger relation

Let $\mathrm{SL}_2\mathbb{C}$ be a matrix group of $(\begin{smallmatrix} a & b \\ c & d \end{smallmatrix})$ with $ad - bc = 1$ and $\mathrm{PSL}_2\mathbb{C}$ be the quotient group factored by $\{\pm(\begin{smallmatrix} 1 & 0 \\ 0 & 1 \end{smallmatrix})\}$. Here, we choose the coefficient ring to be \mathbb{C} of complex numbers, but almost all the arguments in this paper hold for arbitrary algebraically closed fields.

Definition 2.1. An $\mathrm{SL}_2\mathbb{C}$ (resp. $\mathrm{PSL}_2\mathbb{C}$) representation of a link K is a group homomorphism ρ from $\pi_1 K$ to $\mathrm{SL}_2\mathbb{C}$ (resp. $\mathrm{PSL}_2\mathbb{C}$). A non-abelian representation ρ is *parabolic* if $\mathrm{tr}(\rho(m)) = 2$ (resp. ± 2) and $\rho(m) \neq (\begin{smallmatrix} 1 & 0 \\ 0 & 1 \end{smallmatrix})$ (resp. $\pm(\begin{smallmatrix} 1 & 0 \\ 0 & 1 \end{smallmatrix})$) for any meridian m .

Remark 2.2. The definition requires that ρ -image is non-abelian, as the original Riley's definition does [Ril72]. However, we sometimes say about *abelian parabolic representations* just ignoring non-abelian requirement. In fact, abelian parabolic representations are very simple and we will briefly think of these in the next section and compute an example of link case in Section 7.4.

Remark 2.3. If the condition requiring non-trivial meridian is omitted then such a representation may not be boundary-parabolic for a link case. In spite of $\mathrm{tr}(\rho(m)) = 2$, the peripheral image of a link component may have the trivial (parabolic) meridian of $(\begin{smallmatrix} 1 & 0 \\ 0 & 1 \end{smallmatrix})$ and a non-parabolic longitude. So we require the non-triviality for any meridian.

An $\mathrm{SL}_2\mathbb{C}$ -representation ρ naturally induces a $\mathrm{PSL}_2\mathbb{C}$ -representation $[\rho]$ by the composition of the canonical projection $\mathrm{SL}_2\mathbb{C} \rightarrow \mathrm{PSL}_2\mathbb{C}$. Moreover, for parabolic representations, $\rho \mapsto [\rho]$ is a bijection as follows.

Lemma 2.4. Any parabolic $\mathrm{PSL}_2\mathbb{C}$ representation ρ lifts to a parabolic $\mathrm{SL}_2\mathbb{C}$ representation $\tilde{\rho}$ uniquely.

Proof. Consider ρ -images of the Wirtinger generators as $\mathrm{PSL}_2\mathbb{C}$ matrix which satisfy the Wirtinger relations of Figure 1. There are two choices of lifting at each $\tilde{\rho}(m_i)$, i.e., $\mathrm{tr}(\tilde{\rho}(m_i)) = +2$ or -2 . Take a lifting of $\mathrm{tr} = +2$, then all Wirtinger relations are also satisfied in $\mathrm{SL}_2\mathbb{C}$. The uniqueness is obvious since the trace is fixed as $+2$. \square

Therefore, we may focus on $\mathrm{SL}_2\mathbb{C}$ representations in many practical cases. From now on, a *representation* always means a parabolic $\mathrm{SL}_2\mathbb{C}$ -representation unless specified otherwise.

2.2. Character variety. Let P be the set of $\mathrm{SL}_2\mathbb{C}$ matrices of $\mathrm{tr} = 2$, i.e.,

$$P := \{(\begin{smallmatrix} a & b \\ c & d \end{smallmatrix}) \in \mathbb{C}^4 \mid ad - bc = 1 \text{ and } a + d = 2\}.$$

Once we have a knot diagram D , let us define the following set

$$R_{par}^* := R_{par}^*(K) := \{(\mathbf{m}_1, \dots, \mathbf{m}_N) \in P^N \subset \mathbb{C}^{4n} \mid \mathbf{r}_1, \dots, \mathbf{r}_N\}$$

where each bold \mathbf{m}_i stands for a matrix corresponding to each Wirtinger generator m_i of D and each \mathbf{r}_i is also the Wirtinger relator replacing the symbols of m_i with \mathbf{m}_i at each r_i . Therefore, R_{par}^* consists of $\mathrm{SL}_2\mathbb{C}$ -representations of $\mathrm{tr}(\mathbf{m}_i) = 2$. Note that the relations $\{\mathbf{r}_i = 1\}$ is a system of polynomial equations of entries in $\mathrm{SL}_2\mathbb{C}$ matrices and hence the R_{par}^* is Zariski-closed and an affine variety in \mathbb{C}^{4N} by definition.

As we are interested in representations up to conjugation, we let $\overline{R_{par}^*}$ be the quotient by conjugation, $\overline{R_{par}^*} := R_{par}^*/\sim$ where

$$\rho \sim \rho' \iff A\rho A^{-1} = \rho' \text{ for some } A \in \mathrm{SL}_2\mathbb{C}$$

and X_{par}^* be defined by $X_{par}^* := R_{par}^*/\sim$ where

$$\rho \sim \rho' \iff \mathrm{tr}(\rho(a)) = \mathrm{tr}(\rho'(a)) \text{ for all } a \in \pi_1 K.$$

Since the coefficient \mathbb{C} is algebraically closed, the image $\mathrm{Im}(\rho)$ of any reducible representation $\rho \in R_{par}$ is conjugated into $\{(\begin{smallmatrix} 1 & 0 \\ 0 & 1 \end{smallmatrix})\}$ ([Ril72, Section 2]). Thus ρ is abelian if and only if ρ is reducible. Considering the basic setting in [CS83] and the fact that $\pi_1 K$ is generated by conjugations of a single generator, we have several obvious facts as follows.

$$\overline{R_{par}^{ab}} = \overline{R_{par}^{red}} = \{((\begin{smallmatrix} 1 & 0 \\ 0 & 1 \end{smallmatrix}), \dots, (\begin{smallmatrix} 1 & 0 \\ 0 & 1 \end{smallmatrix})), [((\begin{smallmatrix} 1 & 1 \\ 0 & 1 \end{smallmatrix}), \dots, (\begin{smallmatrix} 1 & 1 \\ 0 & 1 \end{smallmatrix}))]\} = \text{two points},$$

$$\overline{R_{par}^{nt}} = \overline{R_{par}^{nab}} \cup \{[((\begin{smallmatrix} 1 & 1 \\ 0 & 1 \end{smallmatrix}), \dots, (\begin{smallmatrix} 1 & 1 \\ 0 & 1 \end{smallmatrix}))]\},$$

$$X_{par}^{ab} = X_{par}^{red} = \text{a singleton of } [\rho] \text{ such that } \mathrm{tr}(\rho(a)) = 2 \text{ for all } a \in \pi_1 K,$$

$$\overline{R_{par}^{nab}} = \overline{R_{par}^{irr}} = X_{par}^{nab} = X_{par}^{irr},$$

$$X_{par}^* = X_{par}^{ab} \cup X_{par}^{nab},$$

where ab , nab , nt , red , and irr stand for *abelian*, *non-abelian*, *non-trivial*, *reducible*, and *irreducible*, respectively and the equalities are just in the set-theoretic sense. In particular, $\overline{R_{par}^{ab}}$ has only two elements from the trivial representation and abelian representations, and $\overline{R_{par}^{nt}}$ is the set of all representations except the trivial representation $\rho_\circ = ((\begin{smallmatrix} 1 & 0 \\ 0 & 1 \end{smallmatrix}), \dots, (\begin{smallmatrix} 1 & 0 \\ 0 & 1 \end{smallmatrix}))$, i.e., the set of only non-trivial abelian representations and non-abelian representations.

Our main concern is the non-abelian parts R_{par}^{nab} and X_{par}^{nab} of R_{par}^* and X_{par}^* , and denote them simply by R_{par} and X_{par} respectively. Now let us define the set of parabolic representations concretely as follows.

Definition 2.5.

$$R_{par} := R_{par}(K) := \{\rho \in R_{par}^*(K) \mid \mathbf{m}_i \neq \mathbf{m}_j \text{ for some } i, j\}$$

Proposition 2.6. R_{par} is the set of parabolic representations.

Proof. Note that ρ is abelian if and only if $\rho(m_i) = \rho(m_j)$ for all $1 \leq i, j \leq N$ since the Wirtinger relation $\rho(r_n) = \mathbf{r}_n = (\begin{smallmatrix} 1 & 0 \\ 0 & 1 \end{smallmatrix})$ becomes $\mathbf{m}_j = \mathbf{m}_k^{\pm 1} \mathbf{m}_i \mathbf{m}_k^{\mp 1} = \mathbf{m}_i$ by the commutativity. The requirement of $\rho(m_i) \neq (\begin{smallmatrix} 1 & 0 \\ 0 & 1 \end{smallmatrix})$ is also obvious. \square

Since $\mathbf{m}_i \neq \mathbf{m}_j$ is a Zariski open condition, the R_{par} is a quasi-affine variety by definition. But we can say R_{par} is an affine variety as follows.

Proposition 2.7. R_{par} is Zariski closed.

Proof. Considering the whole representation variety $R(K)$ in the sense of Culler-Shalen [CS83], it is obvious that $R_{par}^* = (t_m : R(K) \rightarrow \mathbb{C})^{-1}(2)$ where $t_m(\rho) = \text{tr}(\rho(m))$ is a regular function on $R(\pi_1 K)$ for a meridian loop m . For the first eigenvalue μ of $\rho(m)$ for any parabolic representation, $\mu = 1$ and hence μ^2 cannot be zero of the Alexander polynomial $\Delta(t)$ of K because $\Delta(1) = \pm 1$. By [Kla91, Theorem 19], an abelian representation $\rho_{\mu=1}^{ab}$ with $\Delta(\mu^2) \neq 0$ has a neighborhood in $R(K)$ entirely consisting of abelian representations and hence a limit point of parabolic representations cannot be an abelian representation. Since R_{par} is quasi-affine, the closure of R_{par} in the usual topology is Zariski-closed [Mum99, Section I.10] and it completes the proof. \square

Maybe one can think of \mathcal{X}_{par} by GIT quotient for a more elaborated theory. It would be possible to see that the coordinate ring $\mathbb{C}[X_{par}]$ is given by $\mathbb{C}[\mathcal{X}_{par}]_{/\sqrt{0}}$ the quotient by the nilradical. In this paper, we consider only X_{par} , not \mathcal{X}_{par} , and usually in the case when X_{par} is zero-dimensional. For the case of $\dim_{\mathbb{C}}(X_{par}) \neq 0$, every statement is for the zero-dimensional subvariety $X_{par}^{(0)}$ instead of X_{par} .

2.3. Parabolic quandle. In [IK13], A. Inoue and Y. Kabaya introduced parabolic quandle. Notice the subtle difference between our setting here and theirs. They considered $\text{PSL}_2 \mathbb{C}$ representations, but we consider $\text{SL}_2 \mathbb{C}$ representations. Although it seems not to produce any practical difference due to Proposition 2.4, we eventually obtain new results as dealing with the sign choices in the arc-colorings, in contrast to all the previous studies with sign-ambiguity.

Definition 2.8. A *parabolic quandle map* \mathcal{M} into $\text{SL}_2 \mathbb{C}$ -matrices with trace 2 is defined by

$$\mathcal{M} : \mathbb{C}^2 \rightarrow P \quad \text{by } \begin{pmatrix} x \\ y \end{pmatrix} \mapsto \begin{pmatrix} 1 - xy & x^2 \\ -y^2 & 1 + xy \end{pmatrix}. \quad (1)$$

We can check that

Proposition 2.9. \mathcal{M} is surjective and two-to-one except at the origin $\begin{pmatrix} 0 \\ 0 \end{pmatrix}$.

Proof. Any element in P is conjugate to a translation $\begin{pmatrix} 1 & 1 \\ 0 & 1 \end{pmatrix}$ and can be written in the form,

$$\begin{pmatrix} x & z \\ y & w \end{pmatrix} \begin{pmatrix} 1 & 1 \\ 0 & 1 \end{pmatrix} \begin{pmatrix} x & z \\ y & w \end{pmatrix}^{-1} = \begin{pmatrix} 1 - xy & x^2 \\ -y^2 & 1 + xy \end{pmatrix}.$$

The preimage of \mathcal{M} is exactly $\{ \begin{pmatrix} x \\ y \end{pmatrix}, \begin{pmatrix} -x \\ -y \end{pmatrix} \}$. \square

Moreover, \mathcal{M} has an important property as follows.

Lemma 2.10. The parabolic quandle map \mathcal{M} is equivariant under left multiplication and conjugation by any $\text{SL}_2 \mathbb{C}$ matrix A , i.e.

$$\mathcal{M}(Ab) = A\mathcal{M}(b)A^{-1} \text{ for } b \in \mathbb{C}^2 \text{ and } A \in \text{SL}_2 \mathbb{C}.$$

Proof. Straightforward computation. □

Let us adopt usual quandle notations \triangleright and \triangleright^{-1} for the following operation in \mathbb{C}^2 ,

$$a \triangleright b := m(b)^{-1}a \quad \text{and} \quad a \triangleright^{-1} b := m(b)a. \quad (2)$$

Then, one can check that \mathbb{C}^2 with \triangleright satisfy the quandle axioms by Lemma 2.10, i.e.

$$(i) \ a \triangleright a = a, \ (ii) \ (a \triangleright b) \triangleright^{-1} b = a, \ (iii) \ (a \triangleright b) \triangleright c = (a \triangleright c) \triangleright (b \triangleright c) \quad \text{for } a, b, c \in \mathbb{C}^2.$$

Therefore, we let $Q := (\mathbb{C}^2, \triangleright)$ be a *parabolic quandle*.

Remark 2.11. The origin $(0) \in \mathbb{C}^2$ would often cause complication, although it satisfies the quandle axiom just as the other vectors. It corresponds to the identity element in $\text{SL}_2\mathbb{C}$ and always produces the trivial representation which has the same character as abelian parabolic representations. We usually exclude it in practice but we sometimes need to consider the null vector in Q in particular for the link cases as in Section 7.4.

Let us consider a system of parabolic quandle for a given diagram D as follows,

$$Q^* := Q_D^* := \{(a_1, \dots, a_N) \in Q^N \mid r_1, \dots, r_N\} \quad (3)$$

where the relation r_n at crossing c_n is given as in Figure 2.

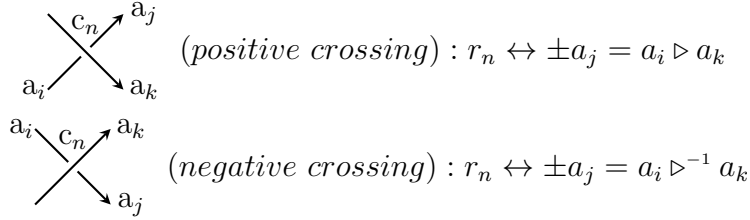


FIGURE 2. Parabolic quandle relation with sign-ambiguity

Q^* is also an affine variety in \mathbb{C}^{2N} since it is the set of solutions to polynomial equations obtained as in Figure 2, which are just equivalent to the Wirtinger relations. Note that the parabolic quandle map m extends to the whole system Q^* onto R_{par}^* by the equivariance given in Lemma 2.10, as follows.

Proposition 2.12. There is a well-defined surjective regular map,

$$m : Q^* \rightarrow R_{par}^* \quad \text{by } a_i \mapsto m(a_i) \text{ for } i = 1, \dots, N.$$

In particular, $|m^{-1}(\rho)| = 2^N$ in R_{par}^{nt} and $m^{-1}(\rho_0) = \{(0, \dots, 0)\}$ with the trivial representation ρ_0 .

Proof. Let us consider a non-trivial representation ρ and its Wirtinger generators

$$(A_1, \dots, A_N) \in R_{par}^{nt}.$$

For any $A_i \in P$, we can find $a_i \in Q$ such that $m(a_i) = A_i$. Then (a_1, \dots, a_N) should be contained in $m^{-1}((A_1, \dots, A_n))$ since the following observation by Lemma 2.10 and (2),

$$\begin{aligned} \pm c = a \triangleright b &\quad \text{if and only if} \quad m(c) = m(b)^{-1}m(a)m(b), \\ \pm c = a \triangleright^{-1} b &\quad \text{if and only if} \quad m(c) = m(b)m(a)m(b)^{-1}. \end{aligned} \quad (4)$$

Moreover, m is always well-defined for any sign-choice of arcs since there are two preimages $+a_i$ and $-a_i$ of the same A_i for each arc. Unless $a_i = \begin{pmatrix} 0 \\ 0 \end{pmatrix}$, it assures that there are 2^N preimages of m where N is the number of arcs in diagram D . \square

Each entry of $a = (a_1, \dots, a_N)$ of \mathcal{Q} assigned to each arc is called an *arc-coloring* traditionally and we also say each arc is colored by Q and each a_i is a *coloring vector*. Remind that we use the notation a_i for an arc and a_i for the corresponding coloring vector. The *associated representation* $\rho_a : \pi_1 K \rightarrow \mathrm{SL}_2 \mathbb{C}$ with respect to an arc-coloring a is obtained by

$$\rho_a(m_i) := m(a_i)$$

where a_i is the *coloring vector* corresponding to Wirtinger generator m_i . Conversely, we say a_ρ is the *associated arc-coloring* with respect to a representation ρ as well. Now, let us define our main concern

$$\mathcal{Q} := m^{-1}(R_{\mathrm{par}})$$

, called a *parabolic quandle system* (with sign-ambiguity) and each element gives a parabolic representation by a regular function m . Obviously \mathcal{Q} is affine variety. One of the goals in the paper is to construct a nice subvariety of \mathcal{Q} with a (set-theoretic) bijection with X_{par} .

Remark 2.13. One can consider \mathcal{Q}_+ naively just as removing the sign-ambiguity from \mathcal{Q} , i.e., replacing \pm with $+$ in Figure 2. In this case, the quandle axioms are still established and m is a well-defined map as well. However, the parabolic quandle map m combined together along D cannot be surjective to R_{par} in general. To be precise, only a boundary-unipotent representation can be obtained through \mathcal{Q}_+ . See Section 3.3 for details.

2.4. Symplectic quandle. We use symplectic quandle to investigate the structure of parabolic quandle equations. The notion of symplectic quandle seems to appear first in [Yet03, NN08] and it was a key feature of computations in [JK20]. Let us begin with the definition of symplectic quandle.

Definition 2.14. Let R be a commutative ring with the unity. A free module M over R equipped with an antisymmetric bilinear form $\langle \cdot, \cdot \rangle : M \times M \rightarrow R$ is called a *symplectic quandle* where the quandle operation \triangleright is given by

$$x \triangleright y := x + \langle x, y \rangle y \quad (5)$$

for all $x, y \in M$.

From the property of the symplectic form $\langle \cdot, \cdot \rangle$, it is easily verified that the operation \triangleright satisfies the quandle axioms and the inverse operation \triangleright^{-1} is given by $x \triangleright^{-1} y = x - \langle x, y \rangle y$. We shall use the symplectic quandle approach for Q with the bilinear form given by the

determinant,

$$\langle a, b \rangle := \det(a, b) \text{ for } a, b \in Q.$$

Then the definition of (5) is exactly the same as in Section 2.3, i.e.,

$$a + \langle a, b \rangle b = a \triangleright b = \mathcal{M}(a)^{-1}b \text{ for } a, b \in Q. \quad (6)$$

Furthermore, we introduce a convenient notation \widehat{a} for a column vector $a \in \mathbb{C}^2$ by

$$\widehat{a} = \widehat{\begin{pmatrix} x \\ y \end{pmatrix}} := (-y, x). \quad (7)$$

Then we have an expression for \mathcal{M} as follows,

$$\mathcal{M}(a) = I + a\widehat{a} \text{ and } \mathcal{M}(a)^{-1} = I - a\widehat{a} \text{ for } a \in Q, \quad (8)$$

where I is the identity matrix $\begin{pmatrix} 1 & 0 \\ 0 & 1 \end{pmatrix}$. From this, we can easily obtain that for $a \in Q$ and $A \in \mathrm{SL}_2\mathbb{C}$,

$$\mathcal{M}(\pm a) = A \text{ if and only if } \mathcal{M}(\pm \sqrt{-1}a) = A^{-1}. \quad (9)$$

Moreover, $\langle a, b \rangle = \widehat{a}b$ for $a, b \in Q$ and hence

$$a \triangleright b = a + (\widehat{a}b)b \text{ and } a \triangleright^{-1} b = a - (\widehat{a}b)b \text{ for } a, b \in Q. \quad (10)$$

Although the symplectic quandle and hat-notation may not be essential mathematically, many parts in quandle computation become convenient practically by using the notations.

2.5. Riley polynomial. Let us briefly review *Riley polynomial*. See [Ril72, Theorem 2] for details. For a two-bridge knot K , the knot group $\pi_1 K$ has a presentation, due to Schubert, of two generators x_1 and x_2 and a single relation. Riley computed all non-abelian parabolic representations ρ as follows. We can put

$$\rho(x_1) = \begin{pmatrix} 1 & 1 \\ 0 & 1 \end{pmatrix} \text{ and } \rho(x_2) = \begin{pmatrix} 1 & 0 \\ -y & 1 \end{pmatrix} \quad (11)$$

up to conjugation and these two matrices satisfy the one matrix relation if and only if there exists a non-abelian representation ρ . In [Ril72, Theorem 2], he showed that the matrix relation is reduced to solving a single integral polynomial $R(y) \in \mathbb{Z}[y]$. Riley named it *representation polynomial* and is now called *Riley polynomial*. We can summarize that Riley established a bijection,

$$\{y \in \mathbb{C} \mid R(y) = 0\} \xrightarrow{\cong} X_{\mathrm{par}} \text{ by } y \mapsto [\rho_y].$$

Furthermore, he showed the followings.

- (1) $R(y)$ is monic.¹
- (2) The constant term is ± 1 .
- (3) $R(y)$ doesn't have any multiple root.

¹In Riley's original notation and definition, $\Lambda(y) = 1 + c_1y + \cdots + c_{\lambda-1}y^{\lambda-1} + (-1)^\lambda y^\lambda \in \mathbb{Z}[y]$, i.e., the constant term is fixed by $+1$. For the generalized Riley polynomial in this paper, the constant term may not be ± 1 in $\mathbb{Z}[y]$. So we define the Riley polynomial $R(y)$ to be with the monic leading coefficient, i.e., $R(y) = (-1)^\lambda \Lambda(y)$.

Recently, Jo and Kim [JK20] showed that some additional properties of $R(y)$ as follows

- (4) Riley polynomial is square-splitting, i.e., $R(u^2) = (-1)^{\deg(g)}g(u)g(-u)$ for $g(u) \in \mathbb{Z}[u]$.
- (5) the root u of y is contained in the trace field $\mathbb{Q}(\text{tr } \rho)$ as a unit of the ring of integers where ρ is the associated representation ρ_y .

We are going to generalize the Riley polynomial to a general knot, not limited to two bridge knot.

3. PARABOLIC QUANDLE WITH SIGN-TYPE

Let us introduce *sign-type* of a parabolic quandle system.

3.1. Sign-types. Let $a = (a_1, \dots, a_N) \in \mathcal{Q}(D)$ of a knot diagram D . We will elaborate parabolic quandle system \mathcal{Q} by specifying a sign choice.

Definition 3.1. A *parabolic quandle system* \mathcal{Q}_ϵ with *sign-type*

$$\epsilon = (\epsilon_1, \dots, \epsilon_N) \in \{\pm 1\}^N$$

is the subset of \mathcal{Q} satisfying the following equation at each crossing c_n for $n = 1, \dots, N$ as in Figure 3. An element of \mathcal{Q}_ϵ is called an *arc-coloring with sign-type* ϵ .

$$\begin{array}{ccc} \begin{array}{c} \text{a}_i \swarrow \text{a}_k \searrow \text{c}_n \text{a}_j \\ \text{a}_i \end{array} & \leftrightarrow \epsilon_n a_j = a_i \triangleright a_k, & \begin{array}{c} \text{a}_i \swarrow \text{c}_n \text{a}_k \searrow \text{a}_j \\ \text{a}_i \end{array} & \leftrightarrow \epsilon_n a_j = a_i \triangleright^{-1} a_k. \end{array}$$

FIGURE 3. Parabolic quandle relation with sign-type

We remark about the redundancy of quandle relation with sign-type. Any single choice of relation r_i in \mathcal{Q} (with sign-ambiguity) is redundant since the single relation r_i among Wirtinger relations is derived from the other relations. The corresponding statement for \mathcal{Q}_ϵ is as follows.

Proposition 3.2. Let $\mathcal{Q}_\epsilon = \{(a_1, \dots, a_N) \in \mathcal{Q}^N \mid r_1^\epsilon, \dots, r_N^\epsilon\}$ where the relations are given by Definition 3.1. Let a_* be an arc-coloring satisfying only $N - 1$ relations with removing r_m^ϵ as follows

$$a_* \in \{(a_1, \dots, a_N) \in \mathcal{Q}^N \mid r_1^\epsilon, \dots, r_{m-1}^\epsilon, r_{m+1}^\epsilon, \dots, r_N^\epsilon\}.$$

In this case, a_* satisfy r_m^ϵ with sign-ambiguity $\epsilon_m \in \{\pm 1\}$ as in Figure 2.

Proof. The corresponding $N - 1$ Wirtinger relations except r_m are satisfied and hence the remaining relation r_m is automatically satisfied with sign-ambiguity. \square

But a_* may or may not satisfy the r_m^ϵ strictly. The obstruction class of ρ affects the sign of ϵ_m . See Section 3.3.

3.2. **Total-sign.** We have several basic properties on sign-type as follows.

Lemma 3.3. (1) \mathcal{Q} is the disjoint union of \mathcal{Q}_ϵ 's, i.e.,

$$\mathcal{Q} = \bigsqcup_{\epsilon \in \{\pm 1\}^N} \mathcal{Q}_\epsilon. \quad (12)$$

(2) For a restriction of \mathcal{M} to \mathcal{Q}_ϵ , i.e., $\mathcal{M}_\epsilon := \mathcal{M}|_{\mathcal{Q}_\epsilon} : \mathcal{Q}_\epsilon \rightarrow R_{par}$, is a 2-to-1 map and the preimage consists of $\{+a, -a\}$ unless \mathcal{Q}_ϵ is an empty set.

Proof. Suppose that $a \in \mathcal{Q}_\epsilon \cap \mathcal{Q}_{\epsilon'}$, i.e., there is the same a for the different ϵ and ϵ' . Then $a_n = -a_n = 0$ since $\epsilon_n \neq \epsilon'_n$ for some n in Figure 3, and all coloring vectors in a must be zero. For the second assertion, it is obvious that if $a \in \mathcal{Q}_\epsilon$ then $-a$ is also in \mathcal{Q}_ϵ . If $a' \in \mathcal{Q}_\epsilon$ different from $\pm a$, there is a pair of a_i and a_j such that $a'_i = \pm a_i$ and $a'_j = \mp a_j$. It implies that the corresponding sign-types are mismatched. It contradicts $a' \in \mathcal{Q}_\epsilon$. \square

Let us consider the set of all possible sign-types for ρ ,

$$S(\rho) := \{\epsilon \in \{+, -\}^N \mid \mathcal{M}_\epsilon^{-1}(\rho) \neq \emptyset\}.$$

Then, we can count the number of sign-types in $S(\rho)$ as follows.

Lemma 3.4. $|S(\rho)| = 2^{N-1}$.

Proof. Consider the surjectivity of \mathcal{M} in Proposition 2.12 and hence $|\mathcal{M}^{-1}(\rho)| = 2^N$. If $\mathcal{M}_\epsilon^{-1}(\rho) \neq \emptyset$ then $|\mathcal{M}_\epsilon^{-1}(\rho)| = 2$ by Lemma 3.3 and hence $|S(\rho)| \geq 2^{N-1}$. As considering $\mathcal{M}_\epsilon^{-1}(\rho) \cap \mathcal{M}_{\epsilon'}^{-1}(\rho) = \emptyset$ for $\epsilon' \neq \epsilon$, we conclude that $|S(\rho)| = 2^{N-1}$. \square

Let us define the *total-sign* $[\epsilon]$ of a sign-type ϵ to be the product of all ϵ_i 's, i.e., $[\epsilon] := \epsilon_1 \epsilon_2 \cdots \epsilon_N$. Then

Proposition 3.5. $[\epsilon] \in \{+1, -1\}$ is constant on $\mathcal{M}^{-1}(\rho)$

Proof. Consider $a = \{a_1, \dots, a_N\}$ and $a' = \{a'_1, \dots, a'_N\}$ in $\mathcal{M}^{-1}(\rho)$. Since $a_i = \pm a'_i$ for each i , we can transform a into a' by a finite sequence of the sign-change of a coloring vector a_i and it suffices to consider only one step. If one change the sign of a single coloring vector a_n into $-a_n$ then the corresponding change ϵ' of the sign-type $\epsilon = (\epsilon_1, \dots, \epsilon_N)$ only occur at two ϵ_i and ϵ_j which are the initial and terminal crossings of the arc a_n . Therefore $[\epsilon] = [\epsilon']$ and it completes the proof without loss of generality. \square

Notation 1. For convenience, from now on, we choose compatible indices for arcs $\{a_1, \dots, a_N\}$ and crossings $\{c_1, \dots, c_N\}$ as taking the ending point of each oriented arc a_i to be c_i . Sometimes, an index $i \in \mathbb{Z}$ is outside the range of $\{1, \dots, N\}$, in which case it is always considered modulo N . The indices of ϵ_i and a_i also follow those of c_i and a_i respectively.

Then we can write down an explicit bijection between \mathcal{Q}_ϵ and $\mathcal{Q}_{\epsilon'}$ as follows.

Proposition 3.6. For any given $\tau \in \{+1, -1\}$, we have

$$\Phi : \mathcal{Q}_\epsilon \rightarrow \mathcal{Q}_{\epsilon'} \text{ by } a_i \mapsto a'_i := \tau a_i \prod_{k=1, \dots, i-1} \epsilon'_k / \epsilon_k$$

with $\tau = a'_1/a_1$.

Proof. For $i = 1$, put $a'_1 = \tau a_1$. Then the formula is obtained by induction on i , due to the quandle relation with sign-type in Definition 3.1. \square

Now we know that the total-sign of ρ is an invariant for ρ and a natural question arises asking the geometric meaning of the total-sign. In the next section, we will prove that the total sign is nothing but the obstruction class of ρ .

3.3. Obstruction classes. For a parabolic representation with $\text{tr}(\rho(m)) = +2$ for a meridian m , the trace of longitude can be $+2$ or -2 , i.e., a parabolic $\text{SL}_2\mathbb{C}$ representation may or may not be boundary-unipotent. It is exactly determined by an *obstruction class* of ρ . Recall that a representation $\tilde{\rho} : \pi_1 K \rightarrow \text{SL}_2\mathbb{C}$ is called *boundary-unipotent* if $\text{tr}(\tilde{\rho}(\gamma)) = 2$ for every loop γ in the boundary of a small tubular neighborhood of K . The obstruction to a boundary-unipotent lifting can be identified with an element of $\{\pm 1\}$, which is referred to as the *obstruction class* of ρ . We refer [CYZ20] for details.

Proposition 3.7. [CYZ20, Proposition 2.2] Let $\rho : \pi_1 K \rightarrow \text{PSL}_2\mathbb{C}$ be a boundary-parabolic representation. The obstruction class $\varepsilon(\rho)$ of ρ is half of $\text{tr}(\tilde{\rho}(\lambda))$ where $\tilde{\rho}$ is a $\text{SL}_2\mathbb{C}$ lifting of ρ and λ is any longitude of K .

For a parabolic $\text{SL}_2\mathbb{C}$ representation ρ , we also refer to the obstruction class of ρ as the obstruction class of $p \circ \rho$ with $p : \text{SL}_2\mathbb{C} \rightarrow \text{PSL}_2\mathbb{C}$.

Theorem 3.8. Let $a = (a_1, \dots, a_N)$ be an arc-coloring of D of sign-type $\epsilon = (\epsilon_1, \dots, \epsilon_N)$ with the associated representation $\rho_a \in R_{\text{par}}$. Then the obstruction class ε of ρ_a is the total-sign of ρ , i.e., $\varepsilon = [\epsilon] = \epsilon_1 \cdots \epsilon_n \in \{\pm 1\}$.

Proof. Suppose arc index is given as in Figure 4. Let m_i be the Wirtinger generator corresponding to an arc a_i . We may assume $a_1 = (\begin{smallmatrix} 1 & 0 \\ 0 & 1 \end{smallmatrix})$, i.e. $\rho_a(m_1) = (\begin{smallmatrix} 1 & 1 \\ 0 & 1 \end{smallmatrix})$ by conjugation since ρ_a is non-trivial.

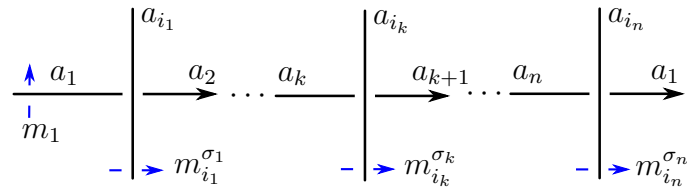


FIGURE 4. Arc index along a diagram D

Let σ_k be the crossing-sign of the k -th crossing from the left in Figure 4. Then the blackboard framed longitude λ_{bf} is given by

$$\lambda_{bf} = m_{i_1}^{\sigma_1} \cdots m_{i_n}^{\sigma_n}.$$

By the definition of ρ_a and using the hat-notation in Section 2.4, we have

$$\begin{aligned} \rho_a(\lambda_{bf}) &= m(a_{i_1})^{\sigma_1} \cdots m(a_{i_n})^{\sigma_n} \\ &= (I + \sigma_1 a_{i_1} \widehat{a_{i_1}}) \cdots (I + \sigma_n a_{i_n} \widehat{a_{i_n}}) \end{aligned}$$

Expanding the above equation, we have

$$\begin{aligned}\rho_a(\lambda_{bf}) &= I + \sum \sigma_{j_1} \sigma_{j_2} \cdots \sigma_{j_k} a_{i_{j_1}} \widehat{a_{i_{j_1}}} a_{i_{j_2}} \widehat{a_{i_{j_2}}} \cdots a_{i_{j_k}} \widehat{a_{i_{j_k}}} \\ &= I + \sum \sigma_{j_1} \sigma_{j_2} \cdots \sigma_{j_k} a_{i_{j_1}} \langle a_{i_{j_1}}, a_{i_{j_2}} \rangle \cdots \langle a_{i_{j_{k-1}}}, a_{i_{j_k}} \rangle \widehat{a_{i_{j_k}}} \\ &= I + \sum \sigma_{j_1} \sigma_{j_2} \cdots \sigma_{j_k} \langle a_{i_{j_1}}, a_{i_{j_2}} \rangle \cdots \langle a_{i_{j_{k-1}}}, a_{i_{j_k}} \rangle a_{i_{j_1}} \widehat{a_{i_{j_k}}}\end{aligned}\quad (13)$$

where the summations are over all possible $1 \leq j_1 < \cdots < j_k \leq n$.

On the other hand, from the definition of type $(\epsilon_1, \dots, \epsilon_n)$ arc-coloring, we have

$$\begin{aligned}\epsilon_2 a_2 &= a_1 + \sigma_1 \langle a_1, a_{i_1} \rangle a_{i_1} \\ \epsilon_3 a_3 &= a_2 + \sigma_2 \langle a_2, a_{i_2} \rangle a_{i_2} \\ &\vdots \\ \epsilon_n a_n &= a_{n-1} + \sigma_{n-1} \langle a_{n-1}, a_{i_{n-1}} \rangle a_{i_{n-1}} \\ \epsilon_1 a_1 &= a_n + \sigma_n \langle a_n, a_{i_n} \rangle a_{i_n}.\end{aligned}$$

Plugging the first equation to ϵ_2 times the second one, we have

$$\begin{aligned}\epsilon_2 \epsilon_3 a_3 &= a_1 + \sigma_1 \langle a_1, a_{i_1} \rangle a_{i_1} + \sigma_2 \langle \epsilon_2 a_2, a_{i_2} \rangle a_{i_2} \\ &= a_1 + \sigma_1 \langle a_1, a_{i_1} \rangle a_{i_1} + \sigma_2 \langle a_1, a_{i_2} \rangle a_{i_2} + \sigma_1 \sigma_2 \langle a_1, a_{i_1} \rangle \langle a_{i_1}, a_{i_2} \rangle a_{i_2}.\end{aligned}$$

Keep plugging till the last equation, we obtain

$$\epsilon_1 \cdots \epsilon_n a_1 = a_1 + \sum \sigma_{j_1} \cdots \sigma_{j_k} \langle a_1, a_{i_{j_1}} \rangle \cdots \langle a_{i_{j_{k-1}}}, a_{i_{j_k}} \rangle a_{i_{j_k}} \quad (14)$$

where the summation is over all possible $1 \leq j_1 < \cdots < j_k \leq n$. Letting $a_i = \binom{c_i}{d_i} \in Q$, we have $d_{i_{j_1}} = \langle a_1, a_{i_{j_1}} \rangle$ and the first entry of the equation (14) gives

$$[\epsilon] = \epsilon_1 \cdots \epsilon_n = 1 + \sum \sigma_{j_1} \cdots \sigma_{j_k} d_{i_{j_1}} \langle a_{i_{j_1}}, a_{i_{j_2}} \rangle \cdots \langle a_{i_{j_{k-1}}}, a_{i_{j_k}} \rangle c_{i_{j_k}}.$$

Recall that $a_1 = \binom{1}{0}$. Also the equation (13) gives

$$\rho_a(\lambda_{bf}) = I + \sum \sigma_{j_1} \sigma_{j_2} \cdots \sigma_{j_k} \langle a_{i_{j_1}}, a_{i_{j_2}} \rangle \cdots \langle a_{i_{j_{k-1}}}, a_{i_{j_k}} \rangle \binom{c_{i_{j_1}}}{d_{i_{j_1}}} (-d_{i_{j_k}} \ c_{i_{j_k}}).$$

Therefore, the (2,2)-entry of $\rho_a(\lambda_{bf})$ is $[\epsilon]$. On the other hand, $\rho_a(\lambda_{bf})$ commutes with $\rho_a(m_1) = \binom{1}{0} \binom{1}{1}$ so it should be of the form $\pm \binom{1}{0} \binom{*}{1}$. Therefore, we have $\text{tr}(\rho_a(\lambda_{bf})) = 2[\epsilon]$ and thus $\varepsilon = [\epsilon]$ finally follows from Proposition 3.7. \square

Remark 3.9. Theorem 3.8 holds for any abelian parabolic representation but doesn't hold for the trivial representation ρ_\circ of null vectors since it has the obstruction class of +1 but an arbitrary choice of ϵ is possible, i.e., we can put $[\epsilon] = \epsilon_1 \cdots \epsilon_N = -1$ for ρ_\circ .

3.4. Parabolic representations. Let us decompose the set of parabolic representations along the obstruction class,

$$R_{\text{par}} = R_{\text{par}}^+ \sqcup R_{\text{par}}^-.$$

The decomposition of Q along sign-type assembles two groups according to the obstruction class as follows,

$$Q = \bigsqcup_{\epsilon \in \{\pm 1\}^N} Q_\epsilon = Q_+ \sqcup Q_-$$

where $\mathcal{Q}_+ := \bigsqcup_{\epsilon_1 \cdots \epsilon_N = +1} \mathcal{Q}_\epsilon$ and $\mathcal{Q}_- := \bigsqcup_{\epsilon_1 \cdots \epsilon_N = -1} \mathcal{Q}_\epsilon$.

All R_{par}^+ , R_{par}^- , and \mathcal{Q}_ϵ are obviously affine varieties.

By the surjectivity of \mathcal{M} in Proposition 2.12, it is also obvious that

$$\begin{aligned} \mathcal{M}_+ &:= \mathcal{M}|_{\mathcal{Q}_+} : \mathcal{Q}_+ \rightarrow R_{par}^+ \text{ and} \\ \mathcal{M}_- &:= \mathcal{M}|_{\mathcal{Q}_-} : \mathcal{Q}_- \rightarrow R_{par}^- \end{aligned}$$

are surjective. These \mathcal{M}_+ and \mathcal{M}_- are 2^N -to-1 maps as well as \mathcal{M} . We can restrict \mathcal{M}_+ (resp. \mathcal{M}_-) to a 2-to-1 surjective map \mathcal{M}_ϵ for any sign-type $\epsilon = (\epsilon_1, \dots, \epsilon_N)$ with $\epsilon_1 \cdots \epsilon_N = +1$ (resp. -1). We summarize this correspondence as follows.

Theorem 3.10. *Let $\rho : \pi_1 K \rightarrow \mathrm{SL}_2 \mathbb{C}$ be a parabolic representation whose obstruction class is $\varepsilon \in \{\pm 1\}$. For any sign-type $\epsilon = (\epsilon_1, \dots, \epsilon_N)$ satisfying $\epsilon_1 \cdots \epsilon_N = \varepsilon$, there exists an arc-coloring $a = (a_1, \dots, a_N)$ of the sign-type ϵ such that the associated representation ρ_a is the given ρ . Moreover, all such arc-colorings are exactly a and $-a$.*

Proof. In Lemma 3.3, we have a surjective 2-to-1 map $\mathcal{M}_\epsilon \rightarrow R_{par}$. By Theorem 3.8, the image of \mathcal{M}_ϵ is contained in R_{par}^ε and the parabolic quandle map restricted to \mathcal{Q}_ϵ ,

$$\mathcal{M}_\epsilon := \mathcal{M}|_{\mathcal{Q}_\epsilon} : \mathcal{Q}_\epsilon \rightarrow R_{par}^\varepsilon$$

which is surjective. Since we have a given representation ρ with the obstruction class ε , R_{par}^ε cannot be empty and we can find a preimage a such that $\mathcal{M}_\epsilon(a) = \rho$. The last assertion is obvious since \mathcal{M}_ϵ is a 2-to-1 map by Lemma 3.3. \square

Therefore, only two pre-specified sign-type ϵ_+ and ϵ_- for $\{+1, -1\}$ obstructions are just enough to consider the whole non-trivial representations. We often denote the chosen two sign-type ϵ_+ and ϵ_- by ϵ_\pm , or simply ϵ if not confused, i.e.,

$$\mathcal{M}_\epsilon := \mathcal{M}_{\epsilon_+} \sqcup \mathcal{M}_{\epsilon_-} : \mathcal{Q}_{\epsilon_+} \sqcup \mathcal{Q}_{\epsilon_-} \rightarrow R_{par}^+ \sqcup R_{par}^- \quad (15)$$

In short, $\mathcal{M}_\epsilon : \mathcal{Q}_\epsilon \rightarrow R_{par}$ and it is exactly 2-1 and surjective.

Now, let us consider $X_{par} = \overline{R_{par}}$, our main concern. Let $\mathcal{Q}_\epsilon / \sim$ be denoted by $\overline{\mathcal{Q}}_\epsilon$ where $a \sim a'$ if and only if $Ba = a'$ for $B \in \mathrm{SL}_2 \mathbb{C}$. Then we have a one-to-one correspondence as follows.

Theorem 3.11. *The induced map*

$$\overline{\mathcal{M}_\epsilon} : \overline{\mathcal{Q}}_\epsilon \longrightarrow X_{par}$$

is well-defined and bijective.

Proof. By Lemma 2.10,

$$\mathcal{M}_\epsilon(Ba) = B\mathcal{M}_\epsilon(a)B^{-1}$$

and hence \mathcal{M}_ϵ is well-defined. By Theorem 3.10, there are two arc-colorings for a representation ρ , i.e.,

$$\{a, -a\} = \mathcal{M}_\epsilon^{-1}(\rho).$$

They are in the same class by the left multiplication, i.e., $-a = \begin{pmatrix} -1 & 0 \\ 0 & -1 \end{pmatrix}a$ and it completes the proof. \square

By this correspondence, we can investigate X_{par} through $\overline{\mathcal{Q}}_\epsilon$ with any convenient sign-type $\epsilon = \epsilon_+ \sqcup \epsilon_-$. We usually use $\epsilon = (1, \dots, \pm 1, \dots, 1)$ with one specified signed crossing for the obstruction $\varepsilon = \epsilon_1 \cdots \epsilon_N = \pm 1$. We will denote such a sign-type of only i -th crossing simply by *sign-type of* $\epsilon_i = \pm 1$.

Finally, we should be careful that this theorem holds only for knots and fails for links.

3.5. Normalization. By choosing two arcs a_i and a_j we have an explicit set-theoretic bijection ,

$$\overline{\mathcal{Q}}_\epsilon \cong \mathcal{Q}_u \sqcup \mathcal{Q}_v$$

in a similar way to [Ril72, Section 2].

Proposition 3.12. Let us fix two arcs a_i and a_j in a knot diagram D . For a parabolic arc-coloring $a \in \overline{\mathcal{Q}}_\epsilon$ there is a unique element in \mathcal{Q}_u with nonzero $u \in \mathbb{C}$ if $\rho_a(m_i m_j) \neq \rho_a(m_j m_i)$ (resp. in \mathcal{Q}_v with nonzero $v \in \mathbb{C}$ if otherwise), where

$$\begin{aligned} \mathcal{Q}_u &= \{(a_1, \dots, a_N) \in \mathcal{Q}_\epsilon \mid a_i = \begin{pmatrix} 1 & \\ 0 & u \end{pmatrix}, a_j = \begin{pmatrix} 0 & \\ u & \end{pmatrix} \text{ for } u \in \mathbb{C}^\times\}, \\ \mathcal{Q}_v &= \{(a_1, \dots, a_N) \in \mathcal{Q}_\epsilon \mid a_i = \begin{pmatrix} 1 & \\ 0 & \end{pmatrix}, a_j = \begin{pmatrix} v & \\ 0 & \end{pmatrix} \text{ for } v \in \mathbb{C}^\times\} / \sim, \end{aligned}$$

where $a \sim a'$ if and only if $\begin{pmatrix} 1 & * \\ 0 & 1 \end{pmatrix} a = a'$.

Proof. By [Ril72, Lemma 1], two matrices in P can be normalized to $\begin{pmatrix} 1 & 1 \\ 0 & 1 \end{pmatrix}$ and $\begin{pmatrix} 1 & 0 \\ x & 1 \end{pmatrix}$ (resp. $\begin{pmatrix} 1 & x \\ 0 & 1 \end{pmatrix}$) for nonzero $x \in \mathbb{C}$. By the correspondence between Q and P we obtain $\begin{pmatrix} 1 & \\ 0 & u \end{pmatrix}$ and $\begin{pmatrix} 0 & \\ u & \end{pmatrix}$ (resp. $\begin{pmatrix} v & \\ 0 & \end{pmatrix}$) for a nonzero $u \in \mathbb{C}$. If we consider left-multiplications by $SL_2 \mathbb{C}$ on the whole $\overline{\mathcal{Q}}_\epsilon$, then the isotropy subgroups are $\{\begin{pmatrix} 1 & 0 \\ 0 & 1 \end{pmatrix}\}$ and $\{\begin{pmatrix} 1 & * \\ 0 & 1 \end{pmatrix}\}$ respectively and it proves the uniqueness. \square

When we compute \mathcal{Q}_v by solving quandle equations in \mathcal{Q}^* , the solution contains abelian representations. So we should remove such a component manually to obtain \mathcal{Q}_v .

Remark 3.13. Note that \mathcal{Q}_u is an algebraic variety by definition and we can see that \mathcal{Q}_v is also algebraic. However, $\overline{\mathcal{Q}}_\epsilon$ and $\mathcal{Q}_u \sqcup \mathcal{Q}_v$ may not be algebraically isomorphic in general, since the non-commuting assumption for \mathcal{Q}_u is not Zariski closed condition.

Nevertheless, this normalization is not only very powerful in computing representations but also is essential in proving Theorem 4.12 later.

4. RILEY POLYNOMIAL AND u -POLYNOMIAL

4.1. Generalized Riley polynomial.

4.1.1. Roots of Riley polynomial. Let us see that, by direct computation from (11), each root of Riley polynomial $R(y)$ comes from

$$y = 2 - \text{tr}(\rho(x_1)\rho(x_2)),$$

where $x_1 x_2 \in \pi_1 K$ is the loop that winds the topmost crossing when we put the two-bridge knot K in Conway normal form.

Let us consider in general

$$y_\gamma(\rho) := 2 - \text{tr} \circ \rho(\gamma)$$

for any $\gamma \in \pi_1 K$. Note that y_γ is a regular function on X_{par} and, in particular, it does not depend on the orientation of γ as follows.

Lemma 4.1. Let γ^{-1} denote a loop $\gamma \in \pi_1 K$ with its opposite orientation. Then we have $y_\gamma = y_{\gamma^{-1}}$.

Proof. From the Cayley-Hamilton equation, we have $A - \text{tr}(A)I + A^{-1} = 0$ for any $A \in \text{SL}_2 \mathbb{C}$. Taking the trace, we have $\text{tr}(A) = \text{tr}(A^{-1})$. \square

In particular, let us consider $y_\gamma(\rho)$ when γ is a crossing loop in Figure 5.

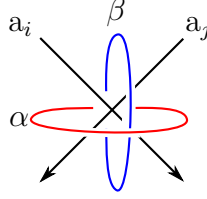


FIGURE 5. Loops winding a crossing.

Let a_i and a_j be arcs at a crossing as in Figure 5. Let m_i and m_j be the Wirtinger generator corresponding to a_i and a_j .

Proposition 4.2. Let α and $\beta \in \pi_1 K$ be loops as in Figure 5. Then we have

- (1) $y_\alpha = y_{m_i m_j} = y_{m_j m_i}$.
- (2) $y_\beta = y_{m_i m_j^{-1}} = y_{m_i^{-1} m_j} = y_{m_j m_i^{-1}} = y_{m_j^{-1} m_i}$.
- (3) $y_\beta = -y_\alpha$.
- (4) $\rho(m_i)\rho(m_j) = \rho(m_j)\rho(m_i)$ if and only if $y_\beta(\rho) = y_\alpha(\rho) = 0$.

Proof. (1) and (2) are straightforward consequences by the Wirtinger generators. By the trace relation, we have

$$\begin{aligned} y_\alpha &= y_{m_1 * m_2} = 2 - \text{tr}(\rho(m_1 m_2)) \\ &= 2 - \text{tr}(\rho(m_1)) \text{tr}(\rho(m_2)) + \text{tr}(\rho(m_1^{-1} m_2)) \\ &= \text{tr}(\rho(m_1^{-1} m_2)) - 2 \\ &= -y_\beta. \end{aligned}$$

On the other hand, any two $\text{SL}_2 \mathbb{C}$ matrices A and B of trace 2 commute if and only if $\text{tr}(AB) = 2$. Therefore, ρ -images of Wirtinger generators around a crossing commute if and only if $y_\beta(\rho) = y_\alpha(\rho) = 0$. \square

Note that the above Proposition holds regardless of over/under information of the crossing.

Definition 4.3. Let us define *y-value* at a crossing c as $y_c(\rho)$, often denoted by y_c or y_{ij} where a_i and a_j are two arcs at the crossing c in Figure 5. Moreover, a *(generalized) Riley*

polynomial $R_c(y)$ at a crossing c is defined by

$$R_c(y) := \prod_{\rho \in X_{par}} (y - y_c(\rho)),$$

where the subindex c is often omitted or replaced by ij if the context is clear.

Remark that we need the assumption that X_{par} is zero-dimensional for the definition of generalized Riley polynomials.

For a two-bridge knot, if we choose a crossing c as the topmost crossing, the ‘generalized’ Riley polynomial $R_c(y)$ coincides with the original Riley’s polynomial. We usually omit the word ‘generalized’ and simply say *Riley polynomial* unless we need to emphasize it.

Remark 4.4. When we define a y -value y_c at a crossing c , there are two choices of crossing loops : α and β in Figure 5. Maybe someone prefers to choose β instead of α and it differs only in sign. Remark that the negative y -value, i.e., y_β choosing β instead of α is exactly the same as *crossing label* in [KKY18, Remark 5.11]. When ρ is a holonomy representation of hyperbolic structure, this y_β is also the same as a geometric quantity, called *intercusp parameter* in [NT16].

Remark 4.5. As we reviewed in Section 2.5, the original Riley polynomial is monic integral and has no multiple root, and the constant term is ± 1 . These properties doesn’t hold anymore. We can easily find an example of a generalized Riley polynomial with multiple roots and non-unit constant term. Let us see 7_4 knot of Section 7.2. The Riley polynomial at the crossing c_5 is $R_{c_5} = (y^3 + y^2 + 13y - 4)(y^2 + y + 1)^2$. We can see the multiple roots and the constant term of -4 . Non-integral Riley polynomial seems to be much rarer and firstly appears in 9_{29} knot. We will prove that, unlike the other properties, the square-splitting property always hold.

4.2. y -value and u -value. An important point is that y -value y_{ij} is the square of the symplectic form $\langle a_i, a_j \rangle$ given by determinant.

Lemma 4.6. Consider an arc-coloring $a = (a_1, \dots, a_N)$ associated to ρ . Let a_i and a_j be two quandle vectors and m_i and m_j be the corresponding Wirtinger generators respectively. Then we have

$$y_{ij} = \langle a_i, a_j \rangle^2.$$

Proof. We have

$$\begin{aligned} y_{ij}(\rho) &= 2 - \text{tr}(\rho(m_i m_j)) \\ &= 2 - \text{tr}(I + a_i \widehat{a}_i)(I + a_j \widehat{a}_j) \\ &= 2 - \text{tr}(I + a_i \widehat{a}_i + a_j \widehat{a}_j + a_i \widehat{a}_i a_j \widehat{a}_j) \\ &= -\widehat{a}_i a_j \text{tr}(a_i \widehat{a}_j) = \langle a_i, a_j \rangle^2. \quad \square \end{aligned}$$

As recalling $\langle a_i, a_j \rangle = \det(a_i a_j)$, we will call the square root of y -value u -value.² More precisely, we define u -value as follows,

²The name y -value or u -value is taken from the variable symbols used in [Ril72, 222p for u , 227p for y]. The assignments here are essentially the same as those of R. Riley originally used, although ‘quandle’ didn’t appear explicitly.

Definition 4.7. $u_{ij} := \langle a_i, a_j \rangle$.

Note that, when we consider of u -value of a representation ρ , the square root u_{ij} of y_{ij} has two choices of $\pm\sqrt{y_{ij}}$ and the u -value $u_{ij} = \langle a_i, a_j \rangle$ also changes according to the sign change of a_i and a_j . If, however, one fixes a sign-type ϵ then $\langle a_i, a_j \rangle$ is well-defined without sign-ambiguity since the signs of a_i and a_j for ρ are changed simultaneously as in Theorem 3.10. When a sign-type ϵ needs to be specified, we use the notation u^ϵ or u_{ij}^ϵ .

Remark 4.8. For a given sign-type ϵ , the u -value u_{ij}^ϵ has no sign-ambiguity. However, even though the sign-type ϵ is determined, u -value u_c at a crossing c has sign-ambiguity because of the following Lemma 4.9. To define u -value at a crossing, we have to decide which two arcs will be used in $\langle a_i, a_j \rangle$ among three arcs around the crossing. We will set the assigning rule for *crossing u-value* so that $u_c^\epsilon = u_{ij}^\epsilon$ where a_i is the under-incoming arc and a_j is the over-arc.

Lemma 4.9. Let three coloring vectors at a crossing c be a , a' and b as in



and ϵ_c is the sign-type at the crossing c . Then,

$$\langle a, b \rangle = \epsilon_c \langle a', b \rangle \quad (16)$$

Proof. $\langle a', b \rangle = \langle \epsilon_c(a \pm (\widehat{ab})b), b \rangle = \epsilon_c \langle a, b \rangle \pm \widehat{ab} \langle b, b \rangle = \epsilon_c \langle a, b \rangle$. \square

4.3. u -polynomials. Let us define a u -polynomial $g(u)$ whose roots are u -values, similar to Riley polynomial $R(y)$ having y -values as roots. Unlike y -values, we need to fix sign-type ϵ to determine u -values without sign-ambiguity.

Lemma 4.10. For a given sign-type ϵ , a u -value u_{ij}^ϵ is well-defined in $\overline{\mathcal{Q}}_\epsilon$ without sign-ambiguity.

Proof. For $B \in \mathrm{SL}_2\mathbb{C}$, $\langle Ba_i, Ba_j \rangle = \det B \det(a_i, a_j) = \langle a_i, a_j \rangle$. \square

Definition 4.11. Let us define a u -polynomial $g(u)$ at a pair of two arcs a_i and a_j by

$$g(u) := g_{ij}^\epsilon(u) := \prod_{a \in X_{par}} (u - u_{ij}^\epsilon), \quad (17)$$

where $a = (a_1, \dots, a_N)$ is an arc-coloring with sign-type ϵ . If a_i and a_j are two arcs at a crossing c in Remark 4.8, the subindex ij of g_{ij}^ϵ is often replaced by c . These subscript ij , c , or ϵ is also often omitted unless confusing.

If $g(u)$ is not contained in $\mathbb{Q}[u]$, this definition would not be meaningful. We prove $g(u) \in \mathbb{Q}[u]$ as follows.

Theorem 4.12. For any i, j , the u -polynomial $g_{ij}(u)$ is contained in $\mathbb{Q}[u]$.

Proof. Let $g(u) = g_{ij}(u)$ and look at the decomposition of $\overline{\mathcal{Q}}_\epsilon$ into \mathcal{Q}_u and \mathcal{Q}_v by Proposition 3.12. We put $a_i = \begin{pmatrix} 1 \\ 0 \end{pmatrix}$, $a_j = \begin{pmatrix} 0 \\ u \end{pmatrix}$ for \mathcal{Q}_u (resp. $a_j = \begin{pmatrix} v \\ 0 \end{pmatrix}$ for \mathcal{Q}_v) and the other colorings

are given indeterminate variables $t_1, t_2, \dots, t_{2(N-2)}$. By the assumption that X_{par} is zero-dimensional, \mathcal{Q}_u and \mathcal{Q}_v are finite sets. Note that each arc-paring u_{ij} in \mathcal{Q}_v becomes zero and hence $g(u) = u^{d'} g'(u)$ with $d' := |\mathcal{Q}_v|$. Each entry u_{ij}, t_1, t_2, \dots of an element of \mathcal{Q}_u is a root of the system of integer coefficient polynomial equations given by quandle relation. They should be algebraic numbers since \mathcal{Q}_u is finite. Note that $Gal(\overline{\mathbb{Q}}/\mathbb{Q})$ acts on \mathcal{Q}_u by a permutation. As considering

$$g_{ij}(u) = \prod(u - u_{ij}) = u^n + C_{n-1}u^{n-1} + \dots + C_1u + C_0$$

and each coefficient C_k is a symmetric function of u_{ij} 's and doesn't change under Galois conjugate. We conclude that $g_{ij} \in \mathbb{Q}[u]$ since every coefficient C_k is invariant under $Gal(\overline{\mathbb{Q}}/\mathbb{Q})$. \square

Let us summarize that by the correspondence of Theorem 3.11 we have

$$\{u \in \mathbb{C} \mid g_c^\epsilon(u) = 0\} \xleftrightarrow{1:1} \{y \in \mathbb{C} \mid R_c(y) = 0\} \xleftrightarrow{1:1} X_{par}. \quad (18)$$

As we mention it in Section 2.2, the higher dimensional part of X_{par} is simply ignored in this paper.

Remark 4.13. Theorem 4.12 and Definition 4.11 works for only knots since the bijection in Theorem 3.11 between $\overline{\mathcal{Q}}_\epsilon$ and X_{par} fails for links. If a_i and a_j belong to different components of the link diagram, both $\pm u_{ij}^\epsilon$ always are contained in $\overline{\mathcal{Q}}_\epsilon$, even though the sign-type ϵ is fixed.

4.4. u -polynomial and sign-types. When the ij index of $g_{ij}^\epsilon(u)$ doesn't need to be specified, We will simply denote it as $g_\epsilon(u)$. By the decomposition along the obstruction class in (15), we obtain

$$g_{\epsilon_\pm}(u) = g_{\epsilon_+}(u)g_{\epsilon_-}(u).$$

Remark that any abelian representation has positive obstruction.

Notation 2. For a given polynomial $g(u)$, let $g^*(u) := (-1)^{\deg(g)}g(-u)$. Then the roots of $g^*(u)$ are $\{-u_1, \dots, -u_n\}$ if and only if the roots of $g(u)$ are $\{u_1, \dots, u_n\}$. The sign correction is for $g^*(u)$ to be monic. This $*$ -notation will be often used in this paper.

Now we consider the change of $g_\epsilon(u)$ for different sign-types.

Theorem 4.14. Let $\epsilon = (\epsilon_1, \dots, \epsilon_N)$ and $\epsilon' = (\epsilon'_1, \dots, \epsilon'_N)$ be two sign-types with the same total-sign, i.e., $\epsilon_1 \cdots \epsilon_N = \epsilon'_1 \cdots \epsilon'_N$. Then

$$g_{ij}^{\epsilon'}(u) = \begin{cases} g_{ij}^\epsilon(u) & \text{for } \epsilon_i \epsilon_{i+1} \dots \epsilon_{j-1} = +\epsilon'_i \epsilon'_{i+1} \dots \epsilon'_{j-1} \\ (g_{ij}^\epsilon)^*(u) & \text{for } \epsilon_i \epsilon_{i+1} \dots \epsilon_{j-1} = -\epsilon'_i \epsilon'_{i+1} \dots \epsilon'_{j-1}. \end{cases}$$

Proof. By the explicit bijection between $\Phi : \mathcal{Q}_\epsilon \rightarrow \mathcal{Q}_{\epsilon'}$ in Proposition 3.6, $a'_i = \tau_{\epsilon_1 \cdots \epsilon_{i-1}}^{\epsilon'_1 \cdots \epsilon'_{i-1}} a_i$. So we have

$$\begin{aligned} \langle a'_i, a'_j \rangle &= \langle \tau_{\epsilon_1 \cdots \epsilon_{i-1}}^{\epsilon'_1 \cdots \epsilon'_{i-1}} a_i, \tau_{\epsilon_1 \cdots \epsilon_{j-1}}^{\epsilon'_1 \cdots \epsilon'_{j-1}} a_j \rangle \\ &= \frac{\epsilon'_i \cdots \epsilon'_{j-1}}{\epsilon_i \cdots \epsilon_{j-1}} \langle a_i, a_j \rangle. \end{aligned} \quad \square$$

Now we can conclude that there are four choices of u -polynomial $g_\epsilon(u) = g_{\epsilon_+}(u)g_{\epsilon_-}(u)$ along the choice of the sign-type ϵ_+ and ϵ_- along each obstruction class,

$$g_{\epsilon_+}(u)g_{\epsilon_-}(u), \quad g_{\epsilon_+}^*(u)g_{\epsilon_-}(u), \quad g_{\epsilon_+}(u)g_{\epsilon_-}^*(u), \quad g_{\epsilon_+}^*(u)g_{\epsilon_-}^*(u),$$

since each $g_{\epsilon_+}(u)$ and $g_{\epsilon_-}(u)$ has two choices of $g_{\epsilon_\pm}(u)$ and $g_{\epsilon_\pm}^*(u)$ along the choices of ϵ_+ and ϵ_- respectively.

Let us consider a canonical choice of sign-type. For positive total-sign, we have the most natural choice, $\epsilon_+ = (+, \dots, +)$ and hence, denote it simply by $g_+(u)$. But for negative total-sign, there is no canonical choice of sign-type. So $g^-(u)$ is not determined whether it is $g_-(u)$ or $g_-^*(u)$, unless the sign-type ϵ_- is specified. However, if we look at a specific crossing, we can think of the following rule to choose a negative sign-type.

Remark 4.15 (Canonical sign-type). Recall Notation 1 and Remark 4.8. In the convention, the index i of incoming arc a_i at a crossing c is the same as the index of the crossing itself, i.e., $c = c_i$. For a crossing c , we have a canonical choice of sign-type ϵ_c as follows,

$$\begin{aligned} \epsilon_c^+ &= (+1, \dots, +1) & \text{and} \\ \epsilon_c^- &= (+1, \dots, -1, \dots, +1) & \text{where } -1 \text{ sign only occurs in } c_i. \end{aligned}$$

Therefore, with the definition of crossing u -value in Remark 4.8, we can define *canonical u -polynomial* at a crossing c without a specified sign-type. As seeing the computation of 8_{18} in Section 8, the canonical u -polynomials have more sensitive properties than Riley polynomials concerning the symmetry of knot, and hence they seem to deserve further study.

We also often omit the symbol ϵ if there is no need to specify a sign-type.

4.4.1. *Square-splitting.* The following proposition is obvious.

Proposition 4.16. For Riley polynomial $R_{ij}(y)$ and u -polynomial $g_{ij}(u)$ at a pair of a_i and a_j with any sign-type ϵ ,

$$R_{ij}(u^2) = g_{ij}(u)g_{ij}^*(u).$$

In particular, $f(u) \mid g_{ij}(u)$ implies $f(u)f^*(u) \mid R_{ij}(u^2)$.

Proof. Recall the definition of $R_{ij}(y)$ and $g_{ij}(u)$ and consider the bijection between the solution sets by (18).

$$\begin{aligned} g_{ij}(u)g_{ij}(-u) &= \prod_{\rho \in X_{par}} (u - u_{ij})(-u - u_{ij}) = \prod_{\rho \in X_{par}} (-u^2 + u_{ij}^2) \\ &= (-1)^{\deg g_{ij}} \prod_{\rho \in X_{par}} (u^2 - y_{ij}) = (-1)^{\deg g_{ij}} R_{ij}(u^2). \end{aligned}$$

The second assertion is obvious from the above statement. \square

Proposition 4.16 comes simply from $y_{ij} = u_{ij}^2$ and it alone doesn't imply $g(u) \in \mathbb{Q}[u]$. However, by combining with Theorem 4.12, we obtain a decomposition theorem immediately as follows.

Theorem 4.17. *A generalized Riley polynomial $R_{ij}(y)$ has rational coefficients and is square-splitting, i.e.,*

$$R_{ij}(u^2) = g_{ij}(u)g_{ij}^*(u) \text{ for } g_{ij}(u) \in \mathbb{Q}[u].$$

Since Riley proved that his polynomial is monic integral, we have the following immediate corollary.

Corollary 4.18. *For a two bridge knot with the top-most or bottom-most generating pair a_i and a_j , $R_{ij}(y) \in \mathbb{Z}[y]$ and hence $R_{ij}(u^2) = g_{ij}(u)g_{ij}^*(u)$ with a monic integral polynomial $g_{ij}(u) \in \mathbb{Z}[u]$.*

Corollary 4.18 was originally proved in [JK20, Theorem 5.1] and Theorem 4.17 can be seen as a generalization of the theorem. Remark that Theorem 4.17 holds only for knots, since Theorem 3.11 is no longer true for links and the proof is also not valid anymore. See the Remark 4.13. We can see a counter-example of the Whitehead link in Section 7.4.

Remark 4.19. Let us compare the generalized Riley polynomial $R_{ij}(y)$ in this paper with the original Riley's polynomial $\Lambda_{\alpha,\beta}(y)$ in [Ril72] and Jo and Kim's polynomial $P_K(u)$ in [JK20]. Since $R_{ij}(y)$ is defined to be monic, $\Lambda_{\alpha,\beta}(y) = (-1)^{\deg(\Lambda_{\alpha,\beta})}R_{ij}(y)$. Note $P_K(u)$ of a knot K , has an additional single u factor, therefore, $P_K(u) = uR_{ij}(u^2)$. Compare [JK20, Theorem 4.9].

5. TRACE FIELD

5.1. Invariant trace fields. The *trace field* $\mathbb{Q}(\text{tr } \rho)$ of a representation ρ is the smallest field containing $\{\text{tr } \circ \rho(g) \mid g \in \pi_1 K\}$ [MR03]. We can also consider the *invariant trace field* of a parabolic representation ρ , which is generated by $\{\text{tr } \circ \rho(g^2) \mid g \in \pi_1 K\}$.

It is well-known that the invariant trace field and the trace field always coincide for a discrete faithful representation of hyperbolic knot complement [MR03, Corollary 4.2.2]. This is also true for any parabolic representation of a knot group as follows.

Proposition 5.1. *For any parabolic representation ρ , the invariant trace field is the same as the trace field $\mathbb{Q}(\text{tr } \rho)$.*

Proof. The ρ -images of $\pi_1 K$ is generated by $\{\rho(m_1), \dots, \rho(m_N)\}$ with m_i 's Wirtinger generators. By the trace relations, the trace field is generated by the ρ -image of the words of at most length 3, $\{m_i, m_i m_j, m_i m_j m_k\}$. By [MR03, Lemma 3.5.9], the invariant trace field is generated by

$$\begin{aligned} \text{tr}^2 \circ \rho(m_i) & \quad \text{for } 1 \leq i \leq N, \\ \text{tr } \circ \rho(m_i m_j) \text{ tr } \circ \rho(m_i) \text{ tr } \circ \rho(m_j), & \quad \text{for } 1 \leq i < j \leq N, \\ \text{tr } \circ \rho(m_i m_j m_k) \text{ tr } \circ \rho(m_i) \text{ tr } \circ \rho(m_j) \text{ tr } \circ \rho(m_k) & \quad \text{for } 1 \leq i < j < k \leq N. \end{aligned}$$

Since $\text{tr } \circ \rho(m_i) = 2$, it is the same generating set as $\mathbb{Q}(\text{tr } \rho)$. \square

One may also study the trace fields of parabolic representations as a commensurable invariant of 3-manifolds but we don't consider this direction in this paper.

5.2. Riley field, u -field, and trace field. For a given knot diagram D and a representation ρ , we have the algebraic number y -value y_{ij} (resp. u -value u_{ij}) for each pair of arcs a_i and a_j . Let $\{y_{ij}\}$ (resp. $\{u_{ij}\}$) be the set of the corresponding y -values (resp. u -values) over all $1 \leq i, j \leq N$. Let us call the number fields $\mathbb{Q}(\{y_{ij}\})$ (resp. $\mathbb{Q}(\{u_{ij}\})$) *Riley field* (resp. *u-field*) generated by $\{y_{ij}\}$ (resp. $\{u_{ij}\}$), where y_{ij} (resp. u_{ij}) is the corresponding root of Riley polynomial $R_{ij}(y)$ (resp. u -polynomial $g_{ij}(u)$).

It is obvious that the Riley field $\mathbb{Q}(\{y_{ij}\})$ is a subfield of the trace field $\mathbb{Q}(\text{tr } \rho)$, but it seems to be unclear whether it can be defined independently of the choice of knot diagram. However, we can assure the invariance of a u -field as follows.

Theorem 5.2. *For a parabolic representation ρ , the u -field $\mathbb{Q}(\{u_{ij}\})$ does not depend on the choice of a knot diagram.*

Proof. Let D' be the knot diagram connected by a single Reidemeister move from D . Let (a_i) and (a'_i) be the parabolic quandles of D and D' respectively, and hence u_{ij} and u'_{ij} denote the u -values of them. The first Reidemeister move doesn't change the set of parabolic quandle vectors $\{a_1, a_2, \dots\}$ and hence the set of u -values $\{u_{11}, u_{12}, \dots, u_{ij}, \dots\}$ as well. Let us denote a'_* the coloring vector of a new arc by the second or the third Reidemeister moves. Because of the quandle relation of $a'_* = a_i \pm \langle a_i, a_j \rangle a_j$ for some i, j , we can always compute a'_* from some arcs a_i and a_j in the previous diagram D . Look at the newly introduced u -values u'_{*k} for $k = 1, \dots, N$. They are obtained by $u'_{*k} = \langle a'_*, a_k \rangle = \langle a_i, a_k \rangle \pm \langle a_i, a_j \rangle \langle a_j, a_k \rangle = u_{ik} \pm u_{ij} u_{jk} \in \mathbb{Q}(\{u_{ij}\})$. Therefore we have $\mathbb{Q}(\{u'_{ij}\}) \subset \mathbb{Q}(\{u_{ij}\})$. Since the role of D and D' can be exchanged, we conclude that $\mathbb{Q}(\{u'_{ij}\}) = \mathbb{Q}(\{u_{ij}\})$. \square

Furthermore, we obtain an inclusion relation between the u -field and the trace field as follows.

Theorem 5.3.

$$\mathbb{Q}(\text{tr } \rho) \subset \mathbb{Q}(\{u_{ij}\})$$

Proof. Because $\text{tr } \rho(m_i) = 2$ and $\text{tr } \rho(m_i m_j) = 2 - (u_{ij})^2$, it is enough to show that $\text{tr } \rho(m_i m_j m_k) \in \mathbb{Q}(\{u_{ij}\})$. Without loss of generality, let us consider $\rho(m_1 m_2 m_3)$ with simplified the indices. Parabolic quandle map \mathcal{M} is surjective, we have quandle vectors a_i such that $\mathcal{M}(a_i) = \rho(m_i)$ for $i = 1, 2, 3$. As recall the hat-notation in Section 2.4, we have $\rho(m_i) = I + a_i \hat{a}_i$ for $i = 1, 2, 3$. Then,

$$\begin{aligned} \rho(m_1 m_2 m_3) &= (I + a_1 \hat{a}_1)(I + a_2 \hat{a}_2)(I + a_3 \hat{a}_3) \\ &= I + a_1 \hat{a}_1 + a_2 \hat{a}_2 + a_3 \hat{a}_3 + a_1 \hat{a}_1 a_2 \hat{a}_2 + a_1 \hat{a}_1 a_3 \hat{a}_3 + a_2 \hat{a}_2 a_3 \hat{a}_3 \\ &\quad + a_1 \hat{a}_1 a_2 \hat{a}_2 a_3 \hat{a}_3. \end{aligned}$$

By the computation of $\text{tr}(a_i \hat{a}_i) = 0$ and $\hat{a}_i a_j = u_{ij} = -\text{tr}(a_i \hat{a}_j)$, we have

$$\text{tr}(\rho(m_1 m_2 m_3)) = 2 - u_{12}^2 - u_{13}^2 - u_{23}^2 - u_{12} u_{23} u_{13} \in \mathbb{Q}(\{u_{ij}\}). \quad \square$$

By the above Theorem 5.2 and Theorem 5.3, we propose the following conjecture.

Conjecture 2. $\mathbb{Q}(\{u_{ij}\}) = \mathbb{Q}(\text{tr } \rho)$

Furthermore, from lots of computer experiments, we also expect the following stronger statement.

Conjecture 3. $\mathbb{Q}(\{y_{ij}\}) = \mathbb{Q}(\{u_{ij}\})$

Conjecture 3 implies not only Conjecture 2, but also $\mathbb{Q}(\{y_{ij}\}) = \mathbb{Q}(\text{tr } \rho)$. Hence it follows that the trace field is generated by the trace of words of only length 2 without worrying the words of length 3. On the other hand, regardless of the truth of $\mathbb{Q}(\{y_{ij}\}) = \mathbb{Q}(\text{tr } \rho)$, it would be independently interesting whether or not Riley field $\mathbb{Q}(\{y_{ij}\})$ is an invariant, i.e., independent of the choice of a knot diagram.

Remark 5.4. We can naturally consider another number fields: $\mathbb{Q}(\{y_c\})$ and $\mathbb{Q}(\{u_c\})$ are generated by all y -values and u -values at each crossing, and these are obviously subfields of $\mathbb{Q}(\{y_{ij}\})$ or $\mathbb{Q}(\{u_{ij}\})$, respectively. Fortunately, we can find an example of 9₃₅ such that $\mathbb{Q}(\{y_c\})$ is a proper subfield of $\mathbb{Q}(\text{tr } \rho)$ and, moreover, is not invariant under the choice of knot diagram. On the other hand, we couldn't find an example of $\mathbb{Q}(\{u_c\}) \neq \mathbb{Q}(\text{tr } \rho)$ for all knot diagrams in [LMar] up to 12 crossings. For u -field case, we suspect that $\mathbb{Q}(\{u_{ij}\}) = \mathbb{Q}(\{u_c\})$ could be true.

Remark 5.5. For two bridge knots, it is easy to see that the trace field is generated by the y -value at the generating pair, i.e., $\mathbb{Q}(\text{tr } \rho) = \mathbb{Q}(y_c)$ where c is the top-most (or bottom-most) crossing. Moreover, in [JK20, Proposition 5.5], it was also shown that $u_c \in \mathbb{Q}(y_c)$ for $y_c = u_c^2$ and hence Conjecture 3 is true for all two bridge knots.

Although the answer to whether $\mathbb{Q}(\{u_{ij}\}) = \mathbb{Q}(\{y_{ij}\})$ could not be obtained, we can obtain an equivalent condition for $\mathbb{Q}(u_{ij}) = \mathbb{Q}(y_{ij})$ which is a kind of ‘local’ statement of Conjecture 3 for each ij pair.

Theorem 5.6. Consider y -value y_{ij} (resp. u -value u_{ij}) at a pair of arcs a_i and a_j , where $y_{ij} = u_{ij}^2$. Let the minimal polynomial of y_{ij} (resp. u_{ij}) be $R_0(y) \in \mathbb{Q}[y]$ (resp. $g_0(u) \in \mathbb{Q}[u]$). Then the followings are equivalent.

- (i) $\mathbb{Q}(u_{ij}) = \mathbb{Q}(y_{ij})$, or equivalently $u_{ij} \in \mathbb{Q}(y_{ij})$.
- (ii) $R_0(u^2)$ is reducible in $\mathbb{Q}[u]$
- (iii) $g_0(u)$ has an odd-degree term.

In particular, $R_0(u^2) = g_0(u)g_0^*(u)$ if the above equivalent conditions hold and $R_0(u^2) = g_0(u)$ otherwise.

Proof. First, suppose that $u_{ij} \in \mathbb{Q}(y_{ij})$. Then $u_{ij} = f(y_{ij})/h(y_{ij})$ where

$$\deg_y f(y), \deg_y h(y) < \deg_y R_0(y).$$

Let $F(u) := uh(u^2) - f(u^2)$. Since

$$\deg_u F(u) \leq 2 \deg_y R_0(y) - 1 < \deg_u R_0(u^2)$$

and $F(u_{ij}) = 0$, $R_0(u^2)$ is never irreducible in $\mathbb{Q}[u]$ and we have (ii). Second, suppose $R_0(u^2)$ is reducible. Then we have $R_0(u^2) = p(u)p^*(u)$ for an irreducible $p(u) \in \mathbb{Q}[u]$ by [Sel56, (9.1)]. Without loss of generality, we can assume $p(u_{ij}) = 0$. Since two monic irreducible

polynomials $p(u)$ and $g_0(u)$ have a common root u_{ij} , $g_0(u) = p(u)$. Suppose that $g_0(u)$ has no odd-degree term and $g_0(u) = q(u^2)$ for some $q(y) \in \mathbb{Q}[y]$, then $R_0(y) = (q(y))^2$ and it contradicts $R_0(y)$ is irreducible. Hence we obtain (iii). Finally, suppose $g_0(u)$ has an odd-degree term. Then $g_0(u) = uf(u^2) + h(u^2)$ with non-zero $f(u)$ and we have $u_{ij} = -h(y_{ij})/f(y_{ij}) \in \mathbb{Q}(y_{ij})$ of (i). It completes the equivalence and the final assertions are trivially obtained in the proof. \square

In the above theorem, the minimal polynomials $R_0(y)$ and $g_0(u)$ are irreducible factors of Riley polynomial $R_{ij}(y)$ and u -polynomial $g_{ij}(u)$, respectively. Note that the degree of $R_{ij}(y)$ and $g_{ij}(u)$ should be the same by the definition. The fact of $\mathbb{Q}(y_{ij}) \neq \mathbb{Q}(u_{ij})$ implies that the Riley polynomial $R_{ij}(y)$ at the pair ij must have multiple roots as follows.

Corollary 5.7. If $R_{ij}(y)$ has distinct roots, then $\mathbb{Q}(y_{ij}) = \mathbb{Q}(u_{ij})$.

Proof. Suppose that $u_{ij} \notin \mathbb{Q}(y_{ij})$. Then the minimal polynomial $g(u)$ of u_{ij} is an even polynomial by (iii) of Theorem 5.6 and hence $g(u) = g^*(u)$. Let us put $g(u) = h(u^2)$. Since $g(u)g^*(u) \mid R_{ij}(u^2)$ by Proposition 4.16, $(h(y))^2$ should divide $R_{ij}(y)$. Therefore $R_{ij}(y)$ has a multiple root and it contradicts the assumption. \square

As an immediate corollary, we obtain the answer to Conjecture 3 for two bridge knots.

Proposition 5.8 (Proposition 5.5 in [JK20]). For two bridge knots, Conjecture 3 is true, i.e., $\mathbb{Q}(\{y_{ij}\}) = \mathbb{Q}(\text{tr } \rho) = \mathbb{Q}(\{u_{ij}\})$.

Proof. Considering a generating crossing c of the two bridge knot, it is clear that $\mathbb{Q}(\{y_{ij}\}) = \mathbb{Q}(y_c)$ and $\mathbb{Q}(\{u_{ij}\}) = \mathbb{Q}(u_c)$ and we have

$$\mathbb{Q}(y_c) = \mathbb{Q}(\{y_{ij}\}) \subset \mathbb{Q}(\text{tr } \rho) \subset \mathbb{Q}(\{u_{ij}\}) = \mathbb{Q}(u_c).$$

By Corollary 5.7 and the fact that $\Lambda_{\alpha,\beta}(y)$ has distinct roots due to Riley, we obtain $\mathbb{Q}(y_c) = \mathbb{Q}(u_c)$ and it completes the proof. \square

6. HOMOMORPHISMS BETWEEN KNOT GROUPS

Let us consider crossing loops α and α' at the crossings c and c' , as in Figure 5, of two knots K and K' respectively. Let $R(y)$ and $R'(y)$ denote Riley polynomials at c and c' of K and K' , respectively.

Theorem 6.1. *If there is a homomorphism $\phi : \pi_1 K \rightarrow \pi_1 K'$ with $\phi(\alpha) = \alpha'$ then any irreducible factor of $R'(y)$ divides $R(y)$. In particular, if ϕ is an epimorphism then $R'(y) \mid R(y)$, and if ϕ is isomorphism then $R'(y) = R(y)$.*

Proof. We have $\phi^* : X_{\text{par}}(K') \rightarrow X_{\text{par}}(K)$ by $\phi^*(\rho') = \rho := \rho' \circ \phi$ for $[\rho'] \in X_{\text{par}}(K')$. Then, the y -value $y_{c'}$ of K' should be the same as y_c of K since $y_{c'}' = 2 - \text{tr } \circ \rho'(\alpha') = 2 - \text{tr } \circ \rho(\alpha) = y_c$. Therefore, the set of $\{y_{c'}(\rho') \mid \rho' \in X'_{\text{par}}(K')\}$ is the subset of $\{y_c(\rho) \mid \rho \in X_{\text{par}}(K)\}$ (with ignoring multiplicity). So we conclude that $R(y) = \prod_{\rho \in X_{\text{par}}(K)} (y - y_c(\rho))$ contains all irreducible factors of $R'(y)$. If ϕ is an epimorphism, ϕ^* becomes monomorphism. So the roots of $R(y)$ should contain all roots of $R'(y)$ concerning the multiplicity and we conclude that the $R'(y)$

itself should divides $R(y)$. If ϕ is an automorphism, $R(y)$ also divides $R'(y)$ and hence $R(y) = R'(y)$. \square

Remark 6.2. Theorem 6.1 holds for oriented links. For knot cases, the Riley polynomial is independent of the orientation of knot and hence the theorem is for unoriented knots. However, for link cases, Riley polynomial depends on the choice of orientation of a link-component since the arc-coloring vector a_i is transformed into ia_i under the change of orientation. This phenomenon will be found in the example of 5_1^2 in Section 7.4.

Example 6.3. Let us see the Riley polynomials of 7_4 knots in Section 7.2. By Theorem 6.1, we can easily prove that there is no homomorphism sending c_5 to any other crossing $R_{c_i}(y)$ with $i \neq 5$ since $R_{c_5}(y)$ is not divided by any factor of $R_{c_i}(y)$ and vice versa.

If X_{par} is decomposed into several irreducible \mathbb{Q} -subvarieties, i.e.,

$$X_{par} = X_{par}^1 \cup X_{par}^2 \cup \cdots \cup X_{par}^n,$$

then $X_{par}^i \cap X_{par}^j = \emptyset$ for all $i \neq j$ because of the assumption that X_{par} is zero-dimensional. Therefore the Riley polynomial $R_c(y)$ is factored as $R_c(y) = R_c^1(y)R_c^2(y) \cdots R_c^n(y) \in \mathbb{Q}[y]$ by definition. Moreover, we can think of a kind of ‘partial’ Riley polynomial $R_c^i(y)$ for a given component X_{par}^i , i.e.

$$R_c^i(y) := \prod_{\rho \in X_{par}^i} (y - y_c(\rho)).$$

Remark that each $R_c^i(y)$ may not be irreducible although X_{par}^i is irreducible. See the example for $R_{c_5}(y)$ of 7_4 in Section 7.2.

The above Theorem 6.1 can be elaborated for each irreducible component X_{par}^i by the same proof.

Theorem 6.4. Let $\phi^* : X_{par}(K') \rightarrow X_{par}(K)$ with $X_{par}(K) = \cup_i X_{par}^i(K)$ and $X_{par}(K') = \cup_j X_{par}^j(K')$. Let $\phi^*(X_{par}^i(K')) \subset X_{par}^j(K)$. Under the same condition of Theorem 6.1, any irreducible factor of the Riley polynomial $R^j(y)$ for $X_{par}^j(K')$ divides $R^i(y)$ for $X_{par}^i(K)$. In particular, if ϕ is epimorphism then $R^j(y) \mid R^i(y)$, and if ϕ is isomorphism then $R^j(y) = R^i(y)$.

We use this theorem to analyze the structure of $X_{par}(8_{18})$ in Section 8.2.

7. COMPUTATIONS

We present several computation examples. The brief procedure is as follows. Firstly, we consider a knot diagram³ with the indexed arcs and crossings. Then we create the system of equation for the normalization in Theorem 3.5 and solve them. Then we obtain X_{par} the set of parabolic representations and their arc-colorings $(a_1, \dots, a_N) \in \mathcal{Q} = \mathcal{Q}_u \cup \mathcal{Q}_v$. As solving the equation, we can also check the sign-types and obtain the obstruction classes by total-sign. To obtain u -polynomials and Riley polynomials, we compute the u -value and y -value at each crossing by finding the polynomial whose roots are u -values and y -values,

³We will use the knot diagrams in Rolfsen table [Rol90].

respectively. Note that from the relation of $R(u^2) = g(u)g^*(u)$, we obtain an u -polynomial just by factoring $R(u^2)$ with up to the choice of $g(u)$ and $g^*(u)$ for each irreducible factor, which depends on the sign-type. For the canonical u -polynomials in the sense of Remark 4.15, we need to change the sign-type for each crossing by Theorem 4.14.

Finally, we compute complex volumes and cusp-shapes of ρ by z -variables (resp. w -variables) of the knot diagram as in [KKY18, Section 6], where these variables can be obtained from the parabolic quandles computed above by the formula of [Cho18, Theorem 3.2] (resp. [Cho16a, Section 2.3]). One can verify these numerical results are consistent with the computations by SnapPy [CDGW] except for the opposite sign of cusp shape since the orientation convention of the boundary torus might be different.

7.1. 4_1 knot. Let us consider a knot diagram and number each arc and crossing respectively as in Figure 6. We have four arc-colorings a_1, a_2, a_3, a_4 and quandle relations at each crossing c_1, c_2, c_3, c_4 .

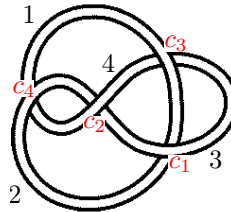


FIGURE 6. Labeling a knot diagram of 4_1 knot.

7.1.1. Quandle equations for \mathcal{Q}_u . Let us begin with $a_1 = \begin{pmatrix} 1 \\ 0 \end{pmatrix}$ and $a_3 = \begin{pmatrix} 0 \\ u \end{pmatrix}$. Then each arc-coloring is computed successively along c_1, c_4 as follows,

$$\begin{aligned} a_2 &\stackrel{c_1}{=} a_1 - \langle a_1, a_3 \rangle a_3 = \begin{pmatrix} 1 \\ -u^2 \end{pmatrix}, \\ a_4 &\stackrel{c_4}{=} a_1 - \langle a_1, a_2 \rangle a_2 = \begin{pmatrix} 1 + u^2 \\ -u^4 \end{pmatrix}. \end{aligned} \tag{19}$$

Note that there are two relations at c_2 and c_3 that have not been used yet. We have all arc-colorings a_i which should satisfy the equation at c_2 as well,

$$a_3 - (a_2 + \langle a_2, a_4 \rangle a_4) = \begin{pmatrix} h_1(u) \\ h_2(u) \end{pmatrix} = 0.$$

By polynomial GCD of h_1 and h_2 , we have

$$g(u) := u^2 + u + 1. \tag{20}$$

Note that every root of $g(u)$ corresponds to each conjugacy class of parabolic representations.

7.1.2. *Obstruction classes.* The final remaining equation at c_3 should be satisfied up to sign,

$$\pm a_4 = a_3 - \langle a_3, a_1 \rangle a_1.$$

We can check that it holds with only the minus sign, not the plus sign and hence every parabolic representation of 4_1 knot has the negative obstruction class. Remark that the $g(u)$ of (20) is the u -polynomial at c_1 with sign-type $(1, 1, -1, 1)$.

7.1.3. *Quandle equations for \mathcal{Q}_v .* As putting $a_1 = \begin{pmatrix} 1 \\ 0 \end{pmatrix}$ and $a_3 = \begin{pmatrix} v \\ 0 \end{pmatrix}$, and solving the equations for \mathcal{Q}_v in a similar way to \mathcal{Q}_u , one can check that there is only a solution of abelian representation. Note that all u -values (and y -values as well) are zero for abelian representations.

7.1.4. *Riley polynomials.* By Lemma 4.6, we obtain y -values from arc-colorings as follows.

$$\begin{aligned} y_{c_1} &= y_{c_3} = u^2, \\ y_{c_2} &= y_{c_4} = u^4. \end{aligned}$$

Note that this y -values do not depend on the choice of sign-type. By the bijection between the roots of $g(u)$ and representations in \mathcal{Q}_u by Theorem 3.11, we compute Riley-polynomials by the following definition,

$$R_{c_i}(y) = \prod_{\rho} (y - y_{c_i}) = \prod_{\mathcal{Q}_u} (y - y_{c_i}) \prod_{\mathcal{Q}_v} (y - y_{c_i}),$$

where \mathcal{Q}_v is an empty set. Then, we obtain

$$R_{c_1} = R_{c_2} = R_{c_3} = R_{c_4} = 1 + y + y^2.$$

7.1.5. *u-polynomials.* First, we compute u -values from the arc-colorings of (19),

$$\begin{aligned} u_{c_1} &= u, & u_{c_2} &= u^2, \\ u_{c_3} &= -u, & u_{c_4} &= -u^2. \end{aligned}$$

Recall that these u -values has the sign-type of $(1, 1, -1, 1)$. So we change the u -values to be with the canonical sign-types at each crossing by using the formula of Theorem 4.14. Then we have

$$\begin{aligned} u_{c_1} &= -u, & u_{c_2} &= u^2, \\ u_{c_3} &= -u, & u_{c_4} &= u^2. \end{aligned}$$

By $g(u) = u^2 + u + 1 = 0$, we also derive canonical u -polynomials as follows,

$$\begin{aligned} g_{c_1} &= g_{c_3} = 1 - u + u^2 \\ g_{c_2} &= g_{c_4} = 1 + u + u^2. \end{aligned}$$

7.1.6. *Complex volumes and Cusp shapes.* The complex volumes and cusp shapes are as follows.

Solution to $g(u)$	$\mathbf{i}(\text{vol} + \mathbf{i}\text{CS})$	Cusp shape
$u = -0.5 - 0.86603\mathbf{i}$	$+ 2.02988\mathbf{i}$	$- 3.46410\mathbf{i}$
$u = -0.5 + 0.86603\mathbf{i}$	$- 2.02988\mathbf{i}$	$+ 3.46410\mathbf{i}$

7.2. 7_4 knot. Let us label each arc and each crossing of 7_4 knot diagram as in Figure 7. We have 7 arc-colorings a_1, \dots, a_7 and quandle relations at each crossing c_1, \dots, c_7 .

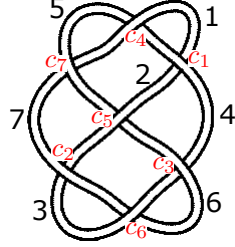


FIGURE 7. Labeling a knot diagram of 7_4 knot.

7.2.1. *Quandle equations for \mathcal{Q}_u .* Let us begin with $a_1 = \begin{pmatrix} 1 \\ 0 \end{pmatrix}$ and $a_4 = \begin{pmatrix} 0 \\ u \end{pmatrix}$. Then, each arc-coloring is computed successively along c_1, c_4, c_5, c_3, c_6 as follows,

$$\begin{aligned}
 a_2 &\stackrel{c_1}{=} a_1 + \langle a_1, a_4 \rangle a_4 = \begin{pmatrix} 1 \\ u^2 \end{pmatrix}, \\
 a_5 &\stackrel{c_4}{=} a_4 + \langle a_4, a_1 \rangle a_1 = \begin{pmatrix} -u \\ u \end{pmatrix}, \\
 a_6 &\stackrel{c_5}{=} a_5 + \langle a_5, a_2 \rangle a_2 = \begin{pmatrix} -u^3 - 2u \\ -u^5 - u^3 + u \end{pmatrix}, \\
 a_3 &\stackrel{c_3}{=} a_4 - \langle a_4, a_6 \rangle a_6 = \begin{pmatrix} u^3(u^2 + 2)^2 \\ u^9 + 3u^7 + u^5 - 2u^3 + u \end{pmatrix}, \\
 a_7 &\stackrel{c_6}{=} a_6 + \langle a_6, a_3 \rangle a_3 = \begin{pmatrix} -u^{11} - 6u^9 - 12u^7 - 8u^5 - u^3 - 2u \\ -u^{13} - 5u^{11} - 7u^9 + 2u^5 - 3u^3 + u \end{pmatrix}.
 \end{aligned} \tag{21}$$

Note that there are two relations at c_2 and c_7 that have not been used yet. We have all arc-colorings a_i which should satisfy the equation at c_2 as well,

$$a_3 - (a_2 + \langle a_2, a_7 \rangle a_7) = \begin{pmatrix} h_1(u) \\ h_2(u) \end{pmatrix} = 0.$$

By polynomial GCD of h_1 and h_2 , we have

$$g(u) := (u^3 + 2u - 1)(u^4 + u^3 + 2u^2 + 2u + 1) = 0. \tag{22}$$

Note that every root of $g(u)$ corresponds to each conjugacy class of parabolic representations.

7.2.2. *Obstruction classes.* The final remaining equation at c_7 should be satisfied up to sign,

$$\pm a_1 = a_7 + \langle a_7, a_5 \rangle a_5.$$

We can check that it holds with only the minus sign, not the plus sign and hence every parabolic representation of 7_4 knot has the negative obstruction class. Remark that the $g(u)$ of (22) is the u -polynomial at c_1 with sign-type $(1, 1, 1, 1, 1, 1, -1)$.

7.2.3. *Arc-coloring vectors.* There are two irreducible components of $g(u) = g_1(u)g_2(u)$ with $g_1(u) = u^3 + 2u - 1$ and $g_2(u) = u^4 + u^3 + 2u^2 + 2u + 1$ and the arc-colorings of each component can be written in the number field $\mathbb{Q}(u_i)$ with a root u_i of g_i as follows.

arc	$g_1(u) = u^3 + 2u - 1$	$g_2(u) = u^4 + u^3 + 2u^2 + 2u + 1$
a_1	$\begin{pmatrix} 1 \\ 0 \end{pmatrix}$	$\begin{pmatrix} 1 \\ 0 \end{pmatrix}$
a_2	$\begin{pmatrix} 1 \\ u^2 \end{pmatrix}$	$\begin{pmatrix} 1 \\ u^2 \end{pmatrix}$
a_3	$\begin{pmatrix} u \\ u^2 - 2u + 1 \end{pmatrix}$	$\begin{pmatrix} 2u^3 + u^2 + 3u + 3 \\ -u^3 - u - 1 \end{pmatrix}$
a_4	$\begin{pmatrix} 0 \\ u \end{pmatrix}$	$\begin{pmatrix} 0 \\ u \end{pmatrix}$
a_5	$\begin{pmatrix} -u \\ u \end{pmatrix}$	$\begin{pmatrix} -u \\ u \end{pmatrix}$
a_6	$\begin{pmatrix} -1 \\ -u^2 - u + 1 \end{pmatrix}$	$\begin{pmatrix} -u^3 - 2u \\ -1 \end{pmatrix}$
a_7	$\begin{pmatrix} -u^2 - 1 \\ u^2 \end{pmatrix}$	$\begin{pmatrix} -u^2 - 1 \\ u^2 \end{pmatrix}$

7.2.4. *Quandle equations for \mathcal{Q}_v .* In a similar way to the case of 4_1 , one can check that there is no representation in \mathcal{Q}_v except abelian representations.

7.2.5. *Riley polynomials.* We obtain y -values as follows.

$$\begin{aligned} y_{c_1} &= y_{c_4} = y_{c_7} = u^2, \\ y_{c_2} &= y_{c_3} = y_{c_6} = u^6 + u^5 + 3u^4 + 2u^3 + 2u^2 + u - 1, \\ y_{c_5} &= u^6 + 2u^4 + u^2. \end{aligned}$$

Since a Riley polynomial $R_{c_i}(y)$ at c_i is the polynomial whose roots are the above y -value y_{c_i} , each $R_{c_i}(y)$ is determined as follows,

$$\begin{aligned} R_{c_1} = R_{c_4} = R_{c_7} = R_{c_2} = R_{c_3} = R_{c_6} &= (y^3 + 4y^2 + 4y - 1)(y^4 + 3y^3 + 2y^2 + 1) \\ R_{c_5} &= (y^3 + y^2 + 13y - 4)(y^2 + y + 1)^2. \end{aligned}$$

7.2.6. *u-polynomials.* First, we compute u -values from the arc-colorings of (21),

$$\begin{aligned} u_{c_1} &= u, \\ u_{c_2} = u_{c_3} &= 2u^2 + u^4, \\ u_{c_4} = u_{c_7} &= -u, \\ u_{c_5} &= -u - u^3, \\ u_{c_6} &= -2u^2 - u^4. \end{aligned}$$

Recall that these u -values have the sign-type of $(1,1,1,1,1,1,-1)$. So we change the u -values to be with the canonical sign-types at each crossing by using the formula of Theorem 4.14. Then we have

$$\begin{aligned} u_{c_1} = u_{c_4} = u_{c_7} &= -u, \\ u_{c_2} = u_{c_3} = u_{c_6} &= -2u^2 - u^4, \\ u_{c_5} &= -u - u^3. \end{aligned}$$

After straightforward computation, we also derive canonical u -polynomials as follows,

$$\begin{aligned} g_{c_1} = g_{c_4} = g_{c_7} = g_{c_2} = g_{c_3} = g_{c_6} &= (1 + 2u + u^3)(1 - 2u + 2u^2 - u^3 + u^4) \\ g_{c_5} &= (2 + 5u + 3u^2 + u^3)(1 - u + u^2)^2. \end{aligned}$$

Note that these canonical u -polynomials respect the diagrammatic symmetry as in the Riley polynomials, whereas the u -polynomials with sign-type $(1, 1, 1, 1, 1, 1, -1)$ does not.

7.2.7. *Complex volumes and Cusp shapes.* The complex volumes and cusp shapes are as follows.

Solution to $g(u)$	$\mathbf{i}(\text{vol} + \mathbf{i}\text{CS})$	Cusp shape
$u = -0.22670 - 1.46771\mathbf{i}$	$9.44074 - 5.13794\mathbf{i}$	$-0.68207 + 3.20902\mathbf{i}$
$u = -0.22670 + 1.46771\mathbf{i}$	$9.44074 + 5.13794\mathbf{i}$	$-0.68207 - 3.20902\mathbf{i}$
$u = 0.45340$	-0.78720	-12.63587
$u = -0.62174 - 0.44060\mathbf{i}$	$3.28987 - 2.02988\mathbf{i}$	$-4 + 3.46410\mathbf{i}$
$u = -0.62174 + 0.44060\mathbf{i}$	$3.28987 + 2.02988\mathbf{i}$	$-4 - 3.46410\mathbf{i}$
$u = 0.12174 - 1.30662\mathbf{i}$	$3.28987 + 2.02988\mathbf{i}$	$-4 - 3.46410\mathbf{i}$
$u = 0.12174 + 1.30662\mathbf{i}$	$3.28987 - 2.02988\mathbf{i}$	$-4 + 3.46410\mathbf{i}$

Let us recall that Chern-Simons invariant is defined by modulo π^2 . The CURVE project [GKR⁺] shows that the Chern-Simons invariant is $0.42887\dots$ which is consistent with $9.44074\dots$ in our table since $0.42887 = -(9.44074 - \pi^2)$. Remark that the Chern-Simons invariants in the CURVE project are computed only modulo $\pi^2/6$, but our computation is modulo π^2 . For example, the complex volume ($\text{vol} + \mathbf{i}\text{CS}$) of geometric representation is $2.02988 - 3.28987\mathbf{i}$ but the CURVE data shows $2.02988\dots$ which agrees modulo $\frac{\pi^2}{6}\mathbf{i}$.

Remark 7.1. The Riley polynomial at c_5 has the Riley polynomial of 4_1 as a factor. We can see that the complex volumes and cusp shapes corresponding to such a factor are closely related to the complex volume and cusp shape of 4_1 as follows.

$$\begin{aligned} \text{vol}_{\mathbb{C}}(\rho) &\equiv \text{vol}_{\mathbb{C}}(4_1) \pmod{\frac{\pi^2}{6}}, \\ \text{cusp}(\rho) &\equiv \text{cusp}(4_1) \pmod{\mathbb{Z}}, \end{aligned}$$

where ρ is a representation of the factor of y^2+y+1 which is the same as the Riley polynomial of 4_1 . This phenomenon with factor-sharing Riley polynomials is observed very often and the geometric interpretation seems worthy of further study.

7.3. 9_{29} knot. Let us label each arc and each crossing of 9_{29} knot diagram as in Figure 8. We have 9 arc-colorings a_1, \dots, a_9 and quandle relations at each crossing c_1, \dots, c_9 .

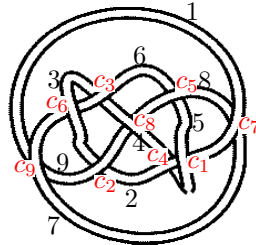


FIGURE 8. Labeling the diagram of 9_{29} knot.

7.3.1. Quandle equations for \mathcal{Q}_u . Let us begin with $a_1 = \begin{pmatrix} 1 \\ 0 \end{pmatrix}$, $a_5 = \begin{pmatrix} 0 \\ u \end{pmatrix}$ and $a_8 = \begin{pmatrix} a \\ b \end{pmatrix}$ with indeterminate variables u, a, b . Then, each arc-coloring is computed successively along $c_1, c_5, c_4, c_3, c_7, c_9$ as follows,

$$\begin{aligned} a_2 &\stackrel{c_1}{=} a_1 + \langle a_1, a_5 \rangle a_5 = \begin{pmatrix} 1 \\ u^2 \end{pmatrix}, \\ a_6 &\stackrel{c_5}{=} a_5 - \langle a_5, a_8 \rangle a_8 = \begin{pmatrix} a^2 u \\ abu + u \end{pmatrix}, \\ a_4 &\stackrel{c_4}{=} a_5 - \langle a_5, a_2 \rangle a_2 = \begin{pmatrix} u \\ u^3 + u \end{pmatrix}, \\ a_3 &\stackrel{c_3}{=} a_4 - \langle a_4, a_6 \rangle a_6 = \begin{pmatrix} a^4 u^5 + a^4 u^3 - a^3 b u^3 - a^2 u^3 + u \\ a^3 b u^5 + a^3 b u^3 - a^2 b^2 u^3 + a^2 u^5 + a^2 u^3 - 2 a b u^3 + u \end{pmatrix}, \\ a_7 &\stackrel{c_7}{=} a_8 + \langle a_8, a_1 \rangle a_1 = \begin{pmatrix} a - b \\ b \end{pmatrix}, \\ a_9 &\stackrel{c_9}{=} a_1 + \langle a_1, a_7 \rangle a_7 = \begin{pmatrix} ab - b^2 + 1 \\ b^2 \end{pmatrix}. \end{aligned} \tag{23}$$

Note that there are three relations at c_2 , c_6 , and c_8 that have not been used yet. We put two of them as follows,

$$a_3 - (a_2 - \langle a_2, a_9 \rangle a_9) = \begin{pmatrix} h_1(u, a, b) \\ h_2(u, a, b) \end{pmatrix} = 0,$$

$$a_7 - (a_6 + \langle a_6, a_3 \rangle a_3) = \begin{pmatrix} h_3(u, a, b) \\ h_4(u, a, b) \end{pmatrix} = 0.$$

7.3.2. Groebner basis. We obtained four equations h_1, h_2, h_3 and $h_4 \in \mathbb{Q}[u, a, b]$ for \mathcal{Q}_u . By using any mathematics software, we have a Groebner basis as the following form,

$$\{g(u), a - f(u), b - h(u)\}, \quad (24)$$

where $g(u) = g_1(u)g_2(u)g_3(u)$ and

$$g_1(u) = u - 1,$$

$$g_2(u) = u^{10} - u^9 + 4u^8 - 7u^7 + 8u^6 - 14u^5 + 11u^4 - 10u^3 + 7u^2 - 2u - 1,$$

$$g_3(u) = u^{16} + 3u^{15} + 10u^{14} + 22u^{13} + 43u^{12} + 73u^{11} + 101u^{10} + 129u^9 + 136u^8$$

$$+ 124u^7 + 100u^6 + 60u^5 + 32u^4 + 12u^3 + 2u^2 + 2u + 1,$$

and $f(u)$ and $g(u)$ are large polynomials of degree 26 in $\mathbb{Q}[u]$. (For example, the leading coefficient and the constant term of $f(u)$ are 15822968441895089 and 80779430690551789.) Now we can see that the decomposition of X_{par} is determined by factoring $g(u)$ and consists of three irreducible components X_{par}^i represented by $g_i(u)$ for $i = 1, 2, 3$.

7.3.3. Quandle equations for \mathcal{Q}_v . For \mathcal{Q}_v , we also have the system of equations by the similar procedure with the initials $a_1 = \begin{pmatrix} 1 \\ 0 \end{pmatrix}$, $a_5 = \begin{pmatrix} v \\ 0 \end{pmatrix}$ and $a_8 = \begin{pmatrix} a \\ b \end{pmatrix}$, and compute the Groebner basis as well. We can check that there are only abelian representations in \mathcal{Q}_v .

7.3.4. Obstruction classes. The last unused equation at c_8 should be satisfied up to sign, which produces the obstruction class as follows.

$$\pm a_9 = a_8 - \langle a_8, a_4 \rangle a_4.$$

We can test which sign holds for each X_{par}^i by putting u, a, b of (24). The single representation in X_{par}^1 is of the only positive obstruction and the other 26 representations in X_{par}^2 and X_{par}^3 are of negative obstruction. Remark that the $g(u)$ of (24) is the u -polynomial at c_1 with sign-type $(1, 1, 1, 1, 1, 1, 1, -1, 1)$.

7.3.5. Riley polynomials. By Lemma 4.6, we obtain y -values as follows.

$$\begin{aligned}
y_{c_1} &= y_{c_4} = u^2, \\
y_{c_2} &= (abu^2 - b^2u^2 - b^2 + u^2)^2, \\
y_{c_3} &= y_{c_6} = u^4(a^2u^2 + a^2 - ab - 1)^2, \\
y_{c_5} &= a^2u^2 \\
y_{c_7} &= y_{c_9} = b^2, \\
y_{c_8} &= u^2(au^2 + a - b)^2.
\end{aligned}$$

Since a Riley polynomial $R_{c_i}(y)$ at c_i is the polynomial whose roots are the above y -value y_{c_i} , each $R_{c_i}(y)$ is determined as follows,

$$\begin{aligned}
R_{c_1} = R_{c_3} = R_{c_4} = R_{c_6} &= (y - 1)(y^{10} + 7y^9 + 18y^8 + 9y^7 - 50y^6 - 110y^5 - 83y^4 - 18y^3 - 13y^2 \\
&\quad - 18y + 1)(y^{16} + 11y^{15} + 54y^{14} + 140y^{13} + 155y^{12} - 143y^{11} - 689y^{10} \\
&\quad - 741y^9 + 198y^8 + 1160y^7 + 926y^6 + 54y^5 - 240y^4 - 56y^3 + 20y^2 + 1) \\
R_{c_2} = R_{c_5} &= \frac{1}{16}(4y - 1)(4y^{10} - 25y^9 + 100y^8 - 198y^7 + 245y^6 - 161y^5 + 29y^4 + 28y^3 \\
&\quad - 14y^2 - y + 1)(y^{16} - 9y^{15} + 66y^{14} - 324y^{13} + 1319y^{12} - 4279y^{11} \\
&\quad + 11631y^{10} - 26121y^9 + 49082y^8 - 76624y^7 + 99630y^6 - 107334y^5 \\
&\quad + 95488y^4 - 68368y^3 + 37044y^2 - 13044y + 2209) \\
R_{c_7} = R_{c_9} &= (y - 1)(y^{10} - 8y^9 + 26y^8 - 17y^7 - 79y^6 + 123y^5 + 236y^4 - 598y^3 \\
&\quad + 349y^2 - 65y + 16)(y^8 - 7y^7 + 19y^6 - 22y^5 + 3y^4 + 14y^3 - 6y^2 \\
&\quad - 4y + 1)^2 \\
R_{c_8} &= y(y^{10} - 3y^9 + 43y^8 - 126y^7 + 731y^6 - 978y^5 + 2754y^4 + 1048y^3 - 639y^2 \\
&\quad - 244y + 64)(y^8 - 3y^7 + 7y^6 - 10y^5 + 11y^4 - 10y^3 + 6y^2 - 4y + 1)^2.
\end{aligned}$$

Note that the factorization of Riley polynomial exactly corresponds to the decomposition of X_{par} and the Riley polynomials for X_{par}^3 has multiple roots at c_7, c_8, c_9 .

7.3.6. *u-polynomials.* First, we compute *u*-values from the arc-colorings of (23),

$$\begin{aligned}
u_{c_1} &= u, \\
u_{c_2} &= -abu^2 + b^2u^2 + b^2 - u^2, \\
u_{c_3} &= u^2 - a^2u^2 + abu^2 - a^2u^4, \\
u_{c_4} &= -u, \\
u_{c_5} &= -au, \\
u_{c_6} &= -u^2 + a^2u^2 - abu^2 + a^2u^4, \\
u_{c_7} &= -b, \\
u_{c_8} &= au - bu + au^3, \\
u_{c_9} &= b.
\end{aligned}$$

Recall that these *u*-values has the sign-type of $(1, 1, 1, 1, 1, 1, 1, -1, 1)$. So we change the *u*-values to be with the canonical sign-types at each crossing by using the formula of Theorem 4.14. Be careful that the transformation formulas into the canonical sign-type are different along the obstruction classes. After straightforward computation, we derive canonical *u*-polynomials as follows,

$$\begin{aligned}
g_{c_1} = g_{c_3} &= (-1 + u)(-1 + 2u + 7u^2 + 10u^3 + 11u^4 + 14u^5 + 8u^6 + 7u^7 + 4u^8 + u^9 + u^{10}) \\
&\quad (1 - 2u + 2u^2 - 12u^3 + 32u^4 - 60u^5 + 100u^6 - 124u^7 + 136u^8 - 129u^9 + 101u^{10} \\
&\quad - 73u^{11} + 43u^{12} - 22u^{13} + 10u^{14} - 3u^{15} + u^{16}) \\
g_{c_4} = g_{c_6} &= (1 + u)(-1 + 2u + 7u^2 + 10u^3 + 11u^4 + 14u^5 + 8u^6 + 7u^7 + 4u^8 + u^9 + u^{10}) \\
&\quad (1 - 2u + 2u^2 - 12u^3 + 32u^4 - 60u^5 + 100u^6 - 124u^7 + 136u^8 - 129u^9 + 101u^{10} \\
&\quad - 73u^{11} + 43u^{12} - 22u^{13} + 10u^{14} - 3u^{15} + u^{16}) \\
g_{c_2} &= \frac{1}{4}(-1 + 2u)(1 - u - 2u^3 - 5u^4 + 7u^5 + 9u^6 - 8u^7 - 4u^8 + 3u^9 + 2u^{10}) \\
&\quad (47 + 136u + 58u^2 - 110u^3 + 40u^4 + 226u^5 + 6u^6 - 146u^7 + 40u^8 + 101u^9 - 19u^{10} \\
&\quad - 33u^{11} + 15u^{12} + 10u^{13} - 4u^{14} - u^{15} + u^{16}) \\
g_{c_5} &= \frac{1}{4}(1 + 2u)(1 - u - 2u^3 - 5u^4 + 7u^5 + 9u^6 - 8u^7 - 4u^8 + 3u^9 + 2u^{10}) \\
&\quad (47 + 136u + 58u^2 - 110u^3 + 40u^4 + 226u^5 + 6u^6 - 146u^7 + 40u^8 + 101u^9 - 19u^{10} \\
&\quad - 33u^{11} + 15u^{12} + 10u^{13} - 4u^{14} - u^{15} + u^{16}) \\
g_{c_7} &= (1 + u)(-1 + 2u + 3u^4 - 2u^5 - 3u^6 + u^7 + u^8)^2(-4 - 11u - 7u^2 + 18u^3 + 12u^4 - 3u^5 \\
&\quad + 5u^6 + u^7 - 4u^8 + u^{10}) \\
g_{c_9} &= (-1 + u)(-1 + 2u + 3u^4 - 2u^5 - 3u^6 + u^7 + u^8)^2(-4 - 11u - 7u^2 + 18u^3 + 12u^4 \\
&\quad - 3u^5 + 5u^6 + u^7 - 4u^8 + u^{10}) \\
g_{c_8} &= u(-1 - 2u + 2u^3 + u^4 - 2u^5 - u^6 + u^7 + u^8)^2(8 - 30u + 41u^2 - 60u^3 + 80u^4 - 30u^5
\end{aligned}$$

$$- 7u^6 + 8u^7 + 3u^8 - 3u^9 + u^{10}).$$

Note that these canonical u -polynomials can be changed for the reflection of the diagram, while Riley polynomials are always preserved under the reflection. Such a phenomenon can also be in the 8_{18} case in Section 8.

7.3.7. Complex volumes and Cusp shapes. The complex volumes and cusp shapes are as in Figure 9. We remark that there is a missing representation of positive obstruction in the CURVE project [GKR⁺].

7.4. Computations for links: 5_1^2 Whitehead link. Essentially, the link cases are similar to the knot case, but we need some modification for the theory. The parabolic quandle map \mathcal{M} without sign-type in Proposition 2.12 is true for any link diagram and the formula computing obstruction class in Theorem 3.8 is also valid if one considers the longitude and the total-sign for each link component. But, $X_{par} \neq \overline{R_{par}^{nt}}$ for link cases and the parabolic quandle system \mathcal{Q}_ϵ with sign-type in Section 3 is not bijective to X_{par} nor $\overline{R_{par}^{nt}}$. In particular, the splitting property of Riley polynomials fails for link cases. Moreover, even if one fixes a sign-type at each crossing, the sign of arc-colorings $\pm(a_1, \dots, a_{N_1})$ and $\pm(b_1, \dots, b_{N_2})$ can be chosen arbitrarily where a_i 's and b_j 's are the arcs in different link components. So we can not define the sign of u -value $u_{ij} = \langle a_i, b_j \rangle$ when the indices i and j are in the different components. We will see these things in the computation of Whitehead link in Section 7.4.

Let us consider a link diagram of the Whitehead link and label each arc and crossing by a_i and c_i respectively as in Figure 10.

7.4.1. Quandle equations for \mathcal{Q}_u . Let us begin with $a_1 = \begin{pmatrix} 1 \\ 0 \end{pmatrix}$ and $a_4 = \begin{pmatrix} 0 \\ u \end{pmatrix}$. Then each arc-coloring is computed successively along c_1, c_4, c_2 as follows,

$$\begin{aligned} a_2 &= a_1 + \langle a_1, a_4 \rangle a_4 = \begin{pmatrix} 1 \\ u^2 \end{pmatrix}, \\ a_5 &= a_4 + \langle a_4, a_1 \rangle a_1 = \begin{pmatrix} -u \\ u \end{pmatrix}, \\ a_3 &= a_2 - \langle a_2, a_5 \rangle a_5 = \begin{pmatrix} u^4 + u^2 + 1 \\ -u^4 \end{pmatrix}. \end{aligned} \tag{25}$$

Note that there are two relations at c_3 and c_5 that have not been used yet.

$$\begin{aligned} a_1 \pm (a_3 - \langle a_3, a_2 \rangle a_2) &= 0, \\ a_4 \pm (a_5 - \langle a_5, a_3 \rangle a_3) &= 0. \end{aligned}$$

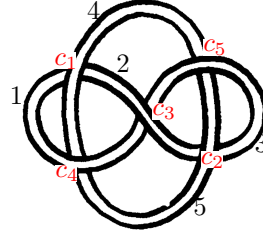
The Whitehead link has two link components and there are 4 kinds of total signs $(-, -)$, $(-, +)$, $(+, -)$ and $(+, +)$ along the choice of sign for each link component, which are determined by the signs of the trace of longitude for the associate representation.

By straightforward computation, the non-abelian representations are only in the $(-, -)$ case and the system of equation is equivalent to $g(u) = u^4 + 2u^2 + 2 = 0$, which has four roots

X_{par}^{irr}		λ	$\mathbb{i}(\text{vol} + \mathbb{i}\text{CS})$	Cusp shape
X_{par}^1	$u = -1$	+	0	$-9/4$
X_{par}^2 (geom)	$u = -0.504 - 1.408i$	+	$10.4508 - 12.2059i$	$7.0577 + 6.5891i$
	$u = -0.504 + 1.408i$		$10.4508 + 12.2059i$	$7.0577 - 6.5891i$
	$u = -0.297 - 1.222i$		$4.7313 - 5.9624i$	$6.5576 + 6.4524i$
	$u = -0.297 + 1.222i$		$4.7313 + 5.9624i$	$6.5576 - 6.4524i$
	$u = -0.231$	-	1.2631	9.0988
	$u = 0.090 - 1.266i$		$8.9245 + 2.3689i$	$11.5357 - 2.9643i$
	$u = 0.090 + 1.266i$		$8.9245 - 2.3689i$	$11.5357 + 2.9643i$
	$u = 0.643 - 0.378i$		$-1.1801 + 1.0383i$	$-4.7369 - 3.7117i$
	$u = 0.643 + 0.378i$		$-1.1801 - 1.0383i$	$-4.7369 + 3.7117i$
X_{par}^3	$u = 1.367$	-	0.5871	12.3229
	$u = -1.142 - 0.105i$		$5.6695 - 6.4435i$	$5.4284 + 5.2942i$
	$u = -1.142 + 0.105i$		$5.6695 + 6.4435i$	$5.4284 - 5.2942i$
	$u = -0.603 - 1.446i$		9.7926	9.8640
	$u = -0.603 + 1.446i$		9.7926	9.8640
	$u = -0.597 - 0.027i$		$1.1305 + 2.5785i$	$0.2771 - 3.5680i$
	$u = -0.597 + 0.027i$		$1.1305 - 2.5785i$	$0.2771 + 3.5680i$
	$u = -0.182 - 1.049i$		4.1349	7.8945
	$u = -0.182 + 1.049i$		4.1349	7.8945
	$u = -0.073 - 1.153i$		$4.3305 - 1.1312i$	$3.4152 + 0.5108i$
	$u = -0.073 + 1.153i$		$4.3305 + 1.1312i$	$3.4152 - 0.5108i$
	$u = 0.281 - 0.319i$		$4.3305 + 1.1312i$	$3.4152 - 0.5108i$
	$u = 0.281 + 0.319i$		$4.3305 - 1.1312i$	$3.4152 + 0.5108i$
	$u = 0.309 - 1.112i$		$1.1305 + 2.5785i$	$0.2771 - 3.5680i$
	$u = 0.309 + 1.112i$		$1.1305 - 2.5785i$	$0.2771 + 3.5680i$
	$u = 0.507 - 1.457i$		$5.6695 + 6.4435i$	$5.4284 - 5.2942i$
	$u = 0.507 + 1.457i$		$5.6695 - 6.4435i$	$5.4284 + 5.2942i$

FIGURE 9. Complex volume and Cusp shape for each representation $\rho \in X_{par}(9_{29})$, where λ is the obstruction class.

$\pm \frac{\sqrt{2\sqrt{2}-2}}{2} \pm \frac{\sqrt{2\sqrt{2}+2}}{2}i$. Note that the correspondence from this normalized quandle solution in \mathcal{Q}_u to \overline{R}_{par} is not bijective but 2-to-1, and hence two roots of u_0 and $-u_0$ of $g(u) = 0$ gives the same representation by the parabolic quandle map in Proposition 2.12. In summary, we can conclude that there are two irreducible representations up to conjugate.

FIGURE 10. Labeling the diagram of 5_1^2 knot.

7.4.2. *Quandle equations for \mathcal{Q}_v .* As putting $a_1 = \begin{pmatrix} 1 \\ 0 \end{pmatrix}$ and $a_4 = \begin{pmatrix} v \\ 0 \end{pmatrix}$, and solving the equations for \mathcal{Q}_v in a similar way to \mathcal{Q}_u , one can check that there is a 1-dimensional solution of abelian representation:

$$a_1 = a_2 = a_3 = \begin{pmatrix} 1 \\ 0 \end{pmatrix}, \quad a_4 = a_5 = \begin{pmatrix} v \\ 0 \end{pmatrix}.$$

We can see that $\overline{R_{par}^{ab}}$ is 1-dimensional, but X_{par}^{ab} is 0-dimensional and a singleton set of constant trace 2 as in the case of knot.

7.4.3. *Abelian representations for 5_1^2 .* For link cases, the abelian representations are more complicated than knot cases. For example, the $\overline{R_{par}^{ab}}(5_1^2)$ has 4 abelian (three 0-dimensional and one 1-dimensional) representation classes up to conjugation as follows,

$$\begin{aligned} \overline{R_{par}^{ab}} = & \{(\mathbf{m}_1, \mathbf{m}_4) \mid \mathbf{m}_1 = \mathbf{m}_4 = \begin{pmatrix} 1 & 0 \\ 0 & 1 \end{pmatrix}; \mathbf{m}_1 = \begin{pmatrix} 1 & 0 \\ 0 & 1 \end{pmatrix}, \mathbf{m}_4 = \begin{pmatrix} 1 & 1 \\ 0 & 1 \end{pmatrix}; \\ & \mathbf{m}_1 = \begin{pmatrix} 1 & 1 \\ 0 & 1 \end{pmatrix}, \mathbf{m}_4 = \begin{pmatrix} 1 & 0 \\ 0 & 1 \end{pmatrix}; \mathbf{m}_1 = \begin{pmatrix} 1 & 1 \\ 0 & 1 \end{pmatrix}, \mathbf{m}_4 = \begin{pmatrix} 1 & v^2 \\ 0 & 1 \end{pmatrix}, \text{ where } v \neq 0\}, \end{aligned}$$

where the other \mathbf{m}_2 , \mathbf{m}_3 , \mathbf{m}_5 are expressed by regular functions of \mathbf{m}_1 and \mathbf{m}_4 . If one considers only the case of non-trivial meridian, i.e., $\rho(\mathbf{m}_i) \neq \begin{pmatrix} 1 & 0 \\ 0 & 1 \end{pmatrix}$ for any i . There is only one component of dimension 1.

7.4.4. *Riley polynomials.* By the formula $y_{ij} = \langle a_i, a_j \rangle^2$, the y -values are

$$\begin{aligned} y(c_1) &= y(c_4) = u^2, \\ y(c_2) &= y(c_5) = -u^2, \\ y(c_3) &= -2u^2 - 2, \end{aligned}$$

and we obtain Riley polynomials as follows

$$\begin{aligned} R_{c_1} &= R_{c_4} = y^2 + 2y + 2, \\ R_{c_2} &= R_{c_5} = y^2 - 2y + 2, \\ R_{c_3} &= y^2 + 4. \end{aligned}$$

As we mentioned in Remark 6.2 that the Riley polynomials for link crossings depend on the choice of the orientation. If we reverse the orientation of the figure-8 component and preserve the orientation of the figure-0 component in Figure 10, then the Riley polynomials

at c_1, c_4 and c_2, c_5 are transformed each other as $y^2 + 2y + 2 \longleftrightarrow y^2 - 2y + 2$, which is from $\langle ia_i, a_j \rangle^2 = -\langle a_i, a_j \rangle^2$ by (9) in Section 2.4. If we apply a π -rotation of the link diagram in Figure 10, then the orientation of the figure-8 component is reversed and we can check that Theorem 6.1 holds for such a π -rotation symmetry.

Note that the square-splitting property is only satisfied for the Riley polynomial R_{c_3} which is the self-crossing in the diagram. The canonical u -polynomial is also only defined at the self-crossing c_3 . The canonical sign-type is $\epsilon_3 = -1$ at the only self-crossing. The corresponding u -values $u_{c_3} = \langle a_3, a_2 \rangle$ are $1 \pm i$ and the canonical u -polynomial is as follows,

$$g_{c_3}(u) = (u - 1 - i)(u - 1 + i) = u^2 - 2u + 2.$$

7.4.5. Complex volumes and Cusp shapes. The complex volumes and cusp shapes are as follows.

$g(u) = 0$	$i(\text{vol} + i\text{CS})$	Cusp shape of L_1	Cusp shape of L_2
$u^2 = -1 - i$	$2.4674 + 3.6638i$	$2 - 2i$	$2 - 2i$
$u^2 = -1 + i$	$2.4674 - 3.6638i$	$2 + 2i$	$2 + 2i$

Remark that, different from knot cases, two conjugacy classes of representations in X_{par} are indicated by the square of the root of $g(u)$. There are two longitudes of L_1 and L_2 where L_1 is the figure-8 component and L_2 is the figure-0 component in Figure 10. We can check that the Chern-Simons invariant is $\pi^2/4$ numerically, but, usually, it is not easy to prove rigorously what the exact value is.

8. COMPUTATION OF $X_{par}(8_{18})$ AND DIAGRAMMATIC SYMMETRY

The 8_{18} is a very symmetrical knot. The structure of $X_{par}(8_{18})$ is exceptionally complicated among the knots with a small number of crossings. In this section, we compute X_{par} and study the behavior for the diagrammatic symmetries.

8.1. Computation. Let us consider a knot diagram of 8_{18} and label each arc and crossing by a_i and c_i as in Figure 11.

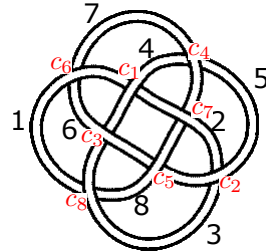


FIGURE 11. A diagram of 8_{18} knot in Rolfsen table.

8.1.1. *Quandle equations for \mathcal{Q}_u .* Let us begin with $a_1 = \begin{pmatrix} 1 \\ 0 \end{pmatrix}$, $a_4 = \begin{pmatrix} 0 \\ u \end{pmatrix}$ and $a_6 = \begin{pmatrix} a \\ b \end{pmatrix}$ with indeterminate variables u, a, b . Then, each arc-coloring is computed successively along c_1, c_6, c_7, c_4, c_2 as follows,

$$\begin{aligned} a_2 &\stackrel{c_1}{=} a_1 - \langle a_1, a_4 \rangle a_4 = \begin{pmatrix} 1 \\ -u^2 \end{pmatrix}, \\ a_7 &\stackrel{c_6}{=} a_6 + \langle a_6, a_1 \rangle a_1 = \begin{pmatrix} a-b \\ b \end{pmatrix}, \\ a_8 &\stackrel{c_7}{=} a_7 - \langle a_7, a_2 \rangle a_2 = \begin{pmatrix} a+au^2-bu^2 \\ b-bu^2-au^4+bu^4 \end{pmatrix}, \\ a_5 &\stackrel{c_4}{=} a_4 + \langle a_4, a_7 \rangle a_7 = \begin{pmatrix} -a^2u+2abu-b^2u \\ u-abu+b^2u \end{pmatrix}, \\ a_3 &\stackrel{c_2}{=} a_2 + \langle a_2, a_5 \rangle a_5 = \begin{pmatrix} 1-a^2u^2+2abu^2+a^3bu^2-b^2u^2-3a^2b^2u^2+3ab^3u^2 \\ -b^4u^2+a^4u^4-4a^3bu^4+6a^2b^2u^4-4ab^3u^4+b^4u^4 \\ -2abu^2+2b^2u^2+a^2b^2u^2-2ab^3u^2+b^4u^2-a^2u^4 \\ +2abu^4+a^3bu^4-b^2u^4-3a^2b^2u^4+3ab^3u^4-b^4u^4 \end{pmatrix}. \end{aligned}$$

When we obtain all colorings, there still remains three unused relations at the crossings c_3, c_5 , and c_8 . We put two of them as follows,

$$\begin{aligned} a_4 - (a_3 - \langle a_3, a_6 \rangle a_6) &= \begin{pmatrix} h_1(u, a, b) \\ h_2(u, a, b) \end{pmatrix} \text{ at } c_3, \\ a_6 - (a_5 - \langle a_5, a_8 \rangle a_8) &= \begin{pmatrix} h_3(u, a, b) \\ h_4(u, a, b) \end{pmatrix} \text{ at } c_5, \end{aligned} \tag{26}$$

and the last equation at c_8 should be satisfied up to sign, which produces the obstruction class.

$$\pm a_1 = a_8 + \langle a_8, a_3 \rangle a_3, \text{ at } c_8. \tag{27}$$

8.1.2. *Primary decomposition.* We obtained four equations h_1, h_2, h_3 , and $h_4 \in \mathbb{Q}[u, a, b]$ for \mathcal{Q}_u and apply primary decomposition algorithms of mathematical softwares⁴. We also have the system of equation for \mathcal{Q}_v by the similar procedure with the initials $a_1 = \begin{pmatrix} 1 \\ 0 \end{pmatrix}$, $a_4 = \begin{pmatrix} v \\ 0 \end{pmatrix}$

and $a_6 = \begin{pmatrix} a \\ b \end{pmatrix}$, and compute the primary decomposition as well.

The irreducible component $X_{par}^2 = \langle -1+v, -1+b \rangle$ (see Figure 12) looks 1-dimensional with coloring of

$$a_1 = a_2 = a_4 = \begin{pmatrix} 1 \\ 0 \end{pmatrix}, a_3 = \begin{pmatrix} 1+a \\ 1 \end{pmatrix}, a_5 = a_6 = a_8 = \begin{pmatrix} a \\ 1 \end{pmatrix}, a_7 = \begin{pmatrix} a-1 \\ 1 \end{pmatrix}.$$

⁴We tested Magma, Maple, Singular and Macaulay2 to do the primary decomposition and compared them. All the results are the same.

Then by multiplication $\begin{pmatrix} 1 & -a \\ 0 & 1 \end{pmatrix} a_i$, we get the following modified solution up to conjugate to the above one:

$$a_1 = a_2 = a_4 = \begin{pmatrix} 1 \\ 0 \end{pmatrix}, a_3 = \begin{pmatrix} 1 \\ 1 \end{pmatrix}, a_5 = a_6 = a_8 = \begin{pmatrix} 0 \\ 1 \end{pmatrix}, a_7 = \begin{pmatrix} -1 \\ 1 \end{pmatrix}.$$

Hence X_{par}^2 becomes 0-dimensional representation.

The results are summarized in Figure 12. \mathcal{Q}_u has 9 irreducible factors where one has positive obstruction and the other remaining 8 cases have negative obstructions. \mathcal{Q}_v has 2 irreducible factors where the one is for abelian representations of X_{par} with positive obstruction and the other one X_{par}^2 has negative obstruction. We index each irreducible component of X_{par} as in Figure 12. Remark that the generating set of X_{par}^i can be differently expressed. For example, X_{par}^7 is determined by the generating set of

$$\langle b^4 - b^3 + 2b + 1, b^3 - 2b^2 + b + u + 2, 2b^3 - 3b^2 + a + b + 3 \rangle.$$

Decomposition	λ	Generating set	
X_{par}	X_{par}^{ab}	+	$\langle v - 1, a - 1, b \rangle$
	X_{par}^1	+	$\langle 1 + u + u^2, 1 + b + u, 1 + a \rangle$
	X_{par}^2	-	$\langle -1 + v, -1 + b \rangle$
	X_{par}^3	-	$\langle -1 + u, -1 + b, a \rangle$
	X_{par}^4	-	$\langle 1 + u, b, 1 + a \rangle$
	X_{par}^5	-	$\langle 1 + u, 1 + b, 1 + a \rangle$
	X_{par}^6	-	$\langle -1 + 2u + u^2 - 2u^3 + u^4, -1 + b + u^2 - u^3, 1 + a \rangle$
	X_{par}^7	-	$\langle 1 + u + u^2, -1 - b + b^2 - u - bu, a - u + bu \rangle$
	X_{par}^8	-	$\langle 3 - 6u + 6u^2 - 3u^3 + u^4, -4 + b + 5u - 3u^2 + u^3, -3 + 3a - u^3 \rangle$
	X_{par}^9	-	$\langle 1 - 2u + u^3 + u^4, -2 + b + u + 2u^2 + u^3, a - 2u - 2u^2 - u^3 \rangle$
	X_{par}^{10}	-	$\langle 1 - 2u + u^3 + u^4, -2 + b + 2u + 3u^2 + 2u^3, 1 + a \rangle$

FIGURE 12. Primary decomposition of $X_{par}(8_{18})$ where λ is the obstruction class.

8.1.3. Riley polynomials. In a similar way to the previous examples, we calculate the y -value at each crossing. We, however, do not explicitly write down them here since the expression itself is not essential and depends on the choice of initial arcs with indeterminate variables u, a, b , and v . As we compute Riley polynomials from the y -values we observe that all Riley

polynomials are the same, i.e.,

$$R_{c_i}(y) = y(y-1)^3(y^2+y+1)^3(y^4-2y^3+7y^2-6y+1) \\ (y^4+3y^3+6y^2+9)(y^4-y^3+6y^2-4y+1)^2,$$

for all $1 \leq i \leq 8$.

Moreover, we compute the corresponding irreducible factors of Riley polynomials for each X_{par}^i , $1 \leq i \leq 10$ in Figure 12.

	X_{par}^1	X_{par}^2	X_{par}^3	X_{par}^4	X_{par}^5	X_{par}^6
c ₁	$1+y+y^2$	y	$-1+y$	$-1+y$	$-1+y$	$1-6y+7y^2-2y^3+y^4$
c ₂	$1+y+y^2$	$-1+y$	$-1+y$	y	$-1+y$	$1-6y+7y^2-2y^3+y^4$
c ₃	$1+y+y^2$	$-1+y$	y	$-1+y$	$-1+y$	$1-6y+7y^2-2y^3+y^4$
c ₄	$1+y+y^2$	$-1+y$	$-1+y$	$-1+y$	y	$1-6y+7y^2-2y^3+y^4$
c ₅	$1+y+y^2$	y	$-1+y$	$-1+y$	$-1+y$	$1-6y+7y^2-2y^3+y^4$
c ₆	$1+y+y^2$	$-1+y$	$-1+y$	y	$-1+y$	$1-6y+7y^2-2y^3+y^4$
c ₇	$1+y+y^2$	$-1+y$	y	$-1+y$	$-1+y$	$1-6y+7y^2-2y^3+y^4$
c ₈	$1+y+y^2$	$-1+y$	$-1+y$	$-1+y$	y	$1-6y+7y^2-2y^3+y^4$

	X_{par}^7	X_{par}^8	X_{par}^9	X_{par}^{10}
c ₁	$(1+y+y^2)^2$	$9+6y^2+3y^3+y^4$	$1-4y+6y^2-y^3+y^4$	$1-4y+6y^2-y^3+y^4$
c ₂	$1-4y+6y^2-y^3+y^4$	$1-4y+6y^2-y^3+y^4$	$(1+y+y^2)^2$	$9+6y^2+3y^3+y^4$
c ₃	$9+6y^2+3y^3+y^4$	$(1+y+y^2)^2$	$1-4y+6y^2-y^3+y^4$	$1-4y+6y^2-y^3+y^4$
c ₄	$1-4y+6y^2-y^3+y^4$	$1-4y+6y^2-y^3+y^4$	$9+6y^2+3y^3+y^4$	$(1+y+y^2)^2$
c ₅	$(1+y+y^2)^2$	$9+6y^2+3y^3+y^4$	$1-4y+6y^2-y^3+y^4$	$1-4y+6y^2-y^3+y^4$
c ₆	$1-4y+6y^2-y^3+y^4$	$1-4y+6y^2-y^3+y^4$	$(1+y+y^2)^2$	$9+6y^2+3y^3+y^4$
c ₇	$9+6y^2+3y^3+y^4$	$(1+y+y^2)^2$	$1-4y+6y^2-y^3+y^4$	$1-4y+6y^2-y^3+y^4$
c ₈	$1-4y+6y^2-y^3+y^4$	$1-4y+6y^2-y^3+y^4$	$9+6y^2+3y^3+y^4$	$(1+y+y^2)^2$

FIGURE 13. Factorization of Riley polynomials along the decomposition of $X_{par}(8_{18})$.

8.1.4. *u-polynomials*. As previously computed examples, we first obtain the *u*-values for the sign-type $(1, 1, 1, 1, 1, 1, 1, -1)$ used to obtain arc-colorings in Section 8.1.1. Then the canonical *u*-polynomials are obtained by transforming into the canonical sign-type at each crossing. Although Riley polynomials are the same at all crossings, there are two kinds of canonical *u*-polynomials as follows,

$$g_{c_i}(u) = (-1+u)^2 u (1+u) (1-u+u^2)^2 (1+u+u^2) (1+2u-u^3+u^4)^2 \\ (-1-2u+u^2+2u^3+u^4) (3+6u+6u^2+3u^3+u^4)$$

for $i = 1, 3, 5, 7$ and

$$g_{c_i}(u) = (-1 + u)u(1 + u)^2(1 - u + u^2)(1 + u + u^2)^2(1 - 2u + u^3 + u^4)^2 \\ (-1 + 2u + u^2 - 2u^3 + u^4)(3 - 6u + 6u^2 - 3u^3 + u^4)$$

for $i = 2, 4, 6, 8$.

Each irreducible factor of u -polynomials for each X_{par}^i , $1 \leq i \leq 10$ in Figure 14.

	X_{par}^1	X_{par}^2	X_{par}^3	X_{par}^4	X_{par}^5	X_{par}^6
c_1	$1 + u + u^2$	u	$1 + u$	$-1 + u$	$-1 + u$	$-1 - 2u + u^2 + 2u^3 + u^4$
c_2	$1 - u + u^2$	$1 + u$	$1 + u$	u	$-1 + u$	$-1 + 2u + u^2 - 2u^3 + u^4$
c_3	$1 + u + u^2$	$1 + u$	u	$-1 + u$	$-1 + u$	$-1 - 2u + u^2 + 2u^3 + u^4$
c_4	$1 - u + u^2$	$1 + u$	$1 + u$	$-1 + u$	u	$-1 + 2u + u^2 - 2u^3 + u^4$
c_5	$1 + u + u^2$	u	$1 + u$	$-1 + u$	$-1 + u$	$-1 - 2u + u^2 + 2u^3 + u^4$
c_6	$1 - u + u^2$	$1 + u$	$1 + u$	u	$-1 + u$	$-1 + 2u + u^2 - 2u^3 + u^4$
c_7	$1 + u + u^2$	$1 + u$	u	$-1 + u$	$-1 + u$	$-1 - 2u + u^2 + 2u^3 + u^4$
c_8	$1 - u + u^2$	$1 + u$	$1 + u$	$-1 + u$	u	$-1 + 2u + u^2 - 2u^3 + u^4$

	X_{par}^7	X_{par}^8	X_{par}^9	X_{par}^{10}
c_1	$(1-u+u^2)^2$	$3+6u+6u^2+3u^3+u^4$	$1+2u-u^3+u^4$	$1+2u-u^3+u^4$
c_2	$1-2u+u^3+u^4$	$1-2u+u^3+u^4$	$(1+u+u^2)^2$	$3-6u+6u^2-3u^3+u^4$
c_3	$3+6u+6u^2+3u^3+u^4$	$(1-u+u^2)^2$	$1+2u-u^3+u^4$	$1+2u-u^3+u^4$
c_4	$1-2u+u^3+u^4$	$1-2u+u^3+u^4$	$3-6u+6u^2-3u^3+u^4$	$(1+u+u^2)^2$
c_5	$(1-u+u^2)^2$	$3+6u+6u^2+3u^3+u^4$	$1+2u-u^3+u^4$	$1+2u-u^3+u^4$
c_6	$1-2u+u^3+u^4$	$1-2u+u^3+u^4$	$(1+u+u^2)^2$	$3-6u+6u^2-3u^3+u^4$
c_7	$3+6u+6u^2+3u^3+u^4$	$(1-u+u^2)^2$	$1+2u-u^3+u^4$	$1+2u-u^3+u^4$
c_8	$1-2u+u^3+u^4$	$1-2u+u^3+u^4$	$3-6u+6u^2-3u^3+u^4$	$(1+u+u^2)^2$

FIGURE 14. Factorization of u -polynomials along the decomposition of $X_{par}(8_{18})$.

8.2. $X_{par}(8_{18})$ and complex volume. As far as the authors know, the complete list of parabolic representations of 8_{18} was not known until this paper. So we would write it down as a proposition.

Proposition 8.1. For 8_{18} knot, there are 26 parabolic representations. In particular, there are 10 irreducible components as \mathbb{Q} -variety and each component has 1, 2 or 4 parabolic representations. The complex volumes and the cusp shapes are listed in Figure 15.

X_{par}^{irr}		λ	$\mathbf{i}(\text{vol} + \mathbf{i}\text{CS})$	Cusp shape	
X_{par}^1	$u = -0.5 - 0.866\mathbf{i}$	+	$+ 4.05977\mathbf{i}$	$- 6.92820\mathbf{i}$	
	$u = -0.5 + 0.866\mathbf{i}$		$- 4.05977\mathbf{i}$	$+ 6.92820\mathbf{i}$	
X_{par}^2	$v = 1$		-1.64493	-6	
X_{par}^3	$u = 1$		-1.64493	-6	
X_{par}^4	$u = -1$		1.64493	6	
X_{par}^5	$u = -1$		1.64493	6	
X_{par}^6 (geom)	$u = -0.883$	-	1.71901	5.40877	
	$u = 0.468$		-1.71901	-5.40877	
	$u = 1.207 - 0.978\mathbf{i}$		-12.3509 \mathbf{i}	+ 7.82655 \mathbf{i}	
	$u = 1.207 + 0.978\mathbf{i}$		+12.3509 \mathbf{i}	- 7.82655 \mathbf{i}	
X_{par}^7	$b = -0.621 - 0.187\mathbf{i}$	-	$-1.64493 - 4.05977\mathbf{i}$	$-6 + 6.92820\mathbf{i}$	
	$b = -0.621 + 0.187\mathbf{i}$		$-1.64493 + 4.05977\mathbf{i}$	$-6 - 6.92820\mathbf{i}$	
	$b = 1.121 - 1.053\mathbf{i}$		$-1.64493 + 4.05977\mathbf{i}$	$-6 - 6.92820\mathbf{i}$	
	$b = 1.121 + 1.053\mathbf{i}$		$-1.64493 - 4.05977\mathbf{i}$	$-6 + 6.92820\mathbf{i}$	
X_{par}^8	$u = 0.648 - 1.498\mathbf{i}$	-	$-1.64493 + 4.05977\mathbf{i}$	$-6 - 6.92820\mathbf{i}$	
	$u = 0.648 + 1.498\mathbf{i}$		$-1.64493 - 4.05977\mathbf{i}$	$-6 + 6.92820\mathbf{i}$	
	$u = 0.851 - 0.632\mathbf{i}$		$-1.64493 - 4.05977\mathbf{i}$	$-6 + 6.92820\mathbf{i}$	
	$u = 0.851 + 0.632\mathbf{i}$		$-1.64493 + 4.05977\mathbf{i}$	$-6 - 6.92820\mathbf{i}$	
X_{par}^9	$u = -1.121 - 1.053\mathbf{i}$	-	$1.64493 + 4.05977\mathbf{i}$	$6 - 6.92820\mathbf{i}$	
	$u = -1.121 + 1.053\mathbf{i}$		$1.64493 - 4.05977\mathbf{i}$	$6 + 6.92820\mathbf{i}$	
	$u = 0.621 - 0.187\mathbf{i}$		$1.64493 - 4.05977\mathbf{i}$	$6 + 6.92820\mathbf{i}$	
	$u = 0.621 + 0.187\mathbf{i}$		$1.64493 + 4.05977\mathbf{i}$	$6 - 6.92820\mathbf{i}$	
X_{par}^{10}	$u = -1.121 - 1.053\mathbf{i}$	-	$1.64493 + 4.05977\mathbf{i}$	$6 - 6.92820\mathbf{i}$	
	$u = -1.121 + 1.053\mathbf{i}$		$1.64493 - 4.05977\mathbf{i}$	$6 + 6.92820\mathbf{i}$	
	$u = 0.621 - 0.187\mathbf{i}$		$1.64493 - 4.05977\mathbf{i}$	$6 + 6.92820\mathbf{i}$	
	$u = 0.621 + 0.187\mathbf{i}$		$1.64493 + 4.05977\mathbf{i}$	$6 - 6.92820\mathbf{i}$	

FIGURE 15. Complex volume and Cusp shape for each representation $\rho \in X_{par}(8_{18})$, where λ is the obstruction class.

To specify each representation in X_{par}^i in Figure 15, the second column of the table indicates the numerical value of u . For X_{par}^8 , the values of b instead of u are given because u does not indicate a single representation in X_{par}^8 .

Remark 8.2. The X_{par}^6 is the geometric component containing a discrete faithful representation ρ_{geo} since the maximal hyperbolic volume 12.3509... appears in the component.

We can verify that the Chern-Simons invariant of ρ_{geo} is zero and it should be so, since 8_{18} is an amphichiral knot. Note that 20 non-geometric representations have non-trivial Chern-Simons invariants all of them being $\pm 1.64493\dots = \pm \pi^2/6$ which is the Chern-Simons invariant of 3_1 . We can observe that, except in the geometric component X_{par}^6 , all complex volumes of $X_{par}(8_{18})$ are of the form $\pm 2\text{vol}(4_1) \pm i\text{CS}(3_1)$. This phenomenon is also found in the non-geometric component of $X_{par}(7_4)$, see Remark 7.1.

Let us say that two representations ρ and ρ' are *essentially equivalent* if $\rho = \rho' \circ \sigma_*$ for an orientation preserving homeomorphism σ of $S^3 \setminus K$ and its induced knot group automorphism $\sigma_* : \pi_1 K \rightarrow \pi_1 K$. Remark that the induced full-back map $\sigma^* : X_{par} \rightarrow X_{par}$ preserves the complex volumes, i.e. $\text{vol}_{\mathbb{C}}(\rho) = \text{vol}_{\mathbb{C}}(\sigma^*(\rho))$, since it is determined by the group homological fundamental class. The 26 representations in X_{par} are classified by the essential equivalence and they are completely determined by the complex volumes as follows.

Theorem 8.3. *For 8_{18} , there are exactly 12 classes of essentially equivalent representations in X_{par} . In particular, the complex volumes completely classify the parabolic representations up to essential equivalence.*

Proof. In X_{par}^1 and X_{par}^6 , all complex volumes are distinct and separate from the other representations. Let us consider an automorphism $\sigma_* : \pi_1 K \rightarrow \pi_1 K$ given by that the crossing labels changed by $i \rightarrow i + 2 \pmod 8$, which comes from nothing but the $\frac{\pi}{2}$ -counterclockwise rotation σ of the diagram. $\sigma^*(X_{par}^2)$ should coincide with some irreducible component of X_{par} . The automorphism σ sends the crossing label c_1 to c_3 , hence the Riley polynomial of X_{par}^2 at c_1 is y and $\sigma^*(X_{par}^2) = X_{par}^3$, since only X_{par}^3 has the same Riley polynomial y at c_3 . Therefore two representations in X_{par}^2 and X_{par}^3 are essentially equivalent. The same holds true for X_{par}^4 and X_{par}^5 .

Similarly, we obtain $\sigma^*(X_{par}^7) = X_{par}^8$ and $\sigma^*(X_{par}^9) = X_{par}^{10}$ by checking the Riley polynomials. \square

Finally, we analyze the structure of X_{par} concerning diagrammatic symmetry. Let us consider two automorphism σ and τ of $\pi_1 K$ from the diagrammatic symmetry. The σ is given by that the crossing labels changed by $i \rightarrow i + 2 \pmod 8$, i.e., $\frac{\pi}{2}$ -counterclockwise rotation of the diagram. The τ is given by that the crossing labels exchanged by $2i \leftrightarrow 2i + 1$, where outer crossings $\{2, 4, 6, 8\}$ transformed into inner crossings $\{3, 5, 7, 1\}$ by an isotopy and reflection.

Note that the σ and τ induce automorphisms σ^* and τ^* of X_{par} and also we can analyze these actions on X_{par} as follows.

Theorem 8.4. (1) $\sigma^* \circ \sigma^* = \tau^* \circ \tau^* = id$

(2) $X_{par}^i = \sigma^*(X_{par}^i) = \tau^*(X_{par}^i)$ for $i = 1, 6$

(3) $\sigma^* : (X_{par}^2, X_{par}^4, X_{par}^7, X_{par}^9) \leftrightarrow (X_{par}^3, X_{par}^5, X_{par}^8, X_{par}^{10})$

(4) $\tau^* : (X_{par}^2, X_{par}^3, X_{par}^7, X_{par}^8) \leftrightarrow (X_{par}^5, X_{par}^4, X_{par}^{10}, X_{par}^9)$.

Proof. All of these arguments are easily derived by Theorem 6.4. \square

REFERENCES

- [Cal06] Danny Calegari, *Real Places and Torus Bundles*, Geometriae Dedicata **118** (2006), no. 1, 209–227 (en), Number: 1. MR 2239457
- [CDGW] Marc Culler, Nathan M. Dunfield, Matthias Goerner, and Jeffrey R. Weeks, *SnapPy, a computer program for studying the geometry and topology of 3-manifolds*, Available at <http://snappy.computop.org>.
- [Cho16a] Jinseok Cho, *Optimistic limit of the colored Jones polynomial and the existence of a solution*, Proc. Amer. Math. Soc. **144** (2016), no. 4, 1803–1814.
- [Cho16b] ———, *Optimistic limits of the colored Jones polynomials and the complex volumes of hyperbolic links*, J. Aust. Math. Soc. **100** (2016), no. 3, 303–337.
- [Cho18] ———, *Quandle theory and the optimistic limits of the representations of link groups*, Pacific J. Math. **295** (2018), no. 2, 329–366.
- [CK] Phillip Choi and Seonhwa Kim, *Parabolic representations of knot group in diagram.site*, 2020–, available at <http://diagram.site>.
- [CKK14] Jinseok Cho, Hyuk Kim, and Seonhwa Kim, *Optimistic limits of Kashaev invariants and complex volumes of hyperbolic links*, J. Knot Theory Ramifications **23** (2014), no. 09, 1450049.
- [CM13] Jinseok Cho and Jun Murakami, *Optimistic limits of the colored Jones polynomials*, J. Korean Math. Soc. **50** (2013), no. 3, 641–693.
- [CS83] Marc Culler and Peter B. Shalen, *Varieties of Group Representations and Splittings of 3-Manifolds*, The Annals of Mathematics **117** (1983), no. 1, 109–146.
- [CYZ20] Jinseok Cho, Seokbeom Yoon, and Christian Zickert, *On the Hikami–Inoue conjecture*, Algebraic & Geometric Topology **20** (2020), no. 1, 279–301.
- [Fra04] Stefano Francaviglia, *Hyperbolic volume of representations of fundamental groups of cusped 3-manifolds*, International Mathematics Research Notices (2004), no. 9, 425–459.
- [GKR⁺] M. Görner, P.-V. Koseleff, F. Rouillier, C. Zickert E., Falbel, S. Garoufalidis, and A. Guilloux, *Curve proect, electronic reference, 2015–*, available at <http://curve.unhyperbolic.org>.
- [GKY19] Dongmin Gang, Seonhwa Kim, and Seokbeom Yoon, *Adjoint Reidemeister torsions from wrapped M5-branes*, arXiv:1911.10718 (2019), to be appeared in Advances in Theoretical and Mathematical Physics.
- [IK13] Ayumu Inoue and Yuichi Kabaya, *Quandle homology and complex volume*, Geom Dedicata **171** (2013), no. 1, 265–292.
- [JK20] Kyeonghee Jo and Hyuk Kim, *Symplectic quandles and parabolic representations of 2-bridge knots and links*, International Journal of Mathematics **31** (2020), no. 10, 2050081.
- [JK22] ———, *Continuant, Chebyshev polynomials, and Riley polynomials*, arXiv:2201.03922v1 (2022).
- [KKY18] Hyuk Kim, Seonhwa Kim, and Seokbeom Yoon, *Octahedral developing of knot complement I: Pseudo-hyperbolic structure*, Geom. Dedicata **197** (2018), 123–172.
- [KKY19] ———, *Octahedral developing of knot complement II: Ptolemy coordinates and applications*, arXiv:1904.06622 [math] (2019).
- [Kla91] Eric Paul Klassen, *Representations of Knot Groups in $SU(2)$* , Transactions of the American Mathematical Society **326** (1991), no. 2, 795–828 (en).
- [KM04] P. B. Kronheimer and T. S. Mrowka, *Dehn surgery, the fundamental group and $SU(2)$* , Mathematical Research Letters **11** (2004), no. 6, 741–754.
- [LMar] Charles Livingston and Allison H. Moore, *Knotinfo: Table of knot invariants*, URL: knotinfo.math.indiana.edu, Current Month Current Year.
- [Mar12] Julien Marché, *Geometric interpretation of simplicial formulas for the Chern-Simons invariant*, Algebr. Geom. Topol. **12** (2012), no. 2, 805–827.
- [MR03] Colin Maclachlan and Alan W. Reid, *The arithmetic of hyperbolic 3-manifolds*, Graduate Texts in Mathematics, vol. 219, Springer-Verlag, New York, 2003.

- [Mum99] David Mumford, *The red book of varieties and schemes*, expanded ed., Lecture Notes in Mathematics, vol. 1358, Springer-Verlag, Berlin, 1999.
- [MY18] Hitoshi Murakami and Yoshiyuki Yokota, *Volume conjecture for knots*, SpringerBriefs in Mathematical Physics, vol. 30, 2018.
- [Neu04] Walter D. Neumann, *Extended Bloch group and the Cheeger-Chern-Simons class*, Geom. Topol. **8** (2004), 413–474.
- [Neu11] ———, *Realizing arithmetic invariants of hyperbolic 3-manifolds*, Interactions between hyperbolic geometry, quantum topology and number theory, Contemp. Math., vol. 541, Amer. Math. Soc., Providence, RI, 2011, pp. 233–246.
- [NN08] Esteban Adam Navas and Sam Nelson, *On symplectic quandles*, Osaka Journal of Mathematics **45** (2008), no. 4, 973–985.
- [NT16] Walter D. Neumann and Anastasiia Tsvietkova, *Intercusp geodesics and the invariant trace field of hyperbolic 3-manifolds*, Proc. Amer. Math. Soc. **144** (2016), no. 2, 887–896.
- [Ril72] Robert Riley, *Parabolic representations of knot groups. I*, Proc. London Math. Soc. (3) **24** (1972), 217–242.
- [Ril75] ———, *Parabolic representations of knot groups. II*, Proc. London Math. Soc. (3) **31** (1975), no. 4, 495–512.
- [Ril13] ———, *A personal account of the discovery of hyperbolic structures on some knot complements*, Expositiones Mathematicae **31** (2013), no. 2, 104–115.
- [Rol90] Dale Rolfsen, *Knots and links*, Mathematics Lecture Series, vol. 7, Publish or Perish, Inc., Houston, TX, 1990.
- [RR21] A. W. Reid and N. Rouse, *Infinitely Many Knots With NonIntegral Trace*, Experimental Mathematics **0** (2021), no. 0, 1–13.
- [Sel56] Ernst S. Selmer, *On the irreducibility of certain trinomials*, Mathematica Scandinavica **4** (1956), no. 0, 287–302.
- [Thu77] William P. Thurston, *The geometry and topology of 3-manifolds*, Lecture notes, Princeton, 1977.
- [TY21] Anh T. Tran and Yoshikazu Yamaguchi, *Adjoint Reidemeister torsions of once-punctured torus bundles*, arXiv:2109.07058 (2021).
- [Yet03] D. N. Yetter, *Quandles and monodromy*, J. Knot Theory Ramifications **12** (2003), no. 4, 523–541.
- [Zic09] Christian K. Zickert, *The volume and Chern-Simons invariant of a representation*, Duke Math. J. **150** (2009), no. 3, 489–532.